Journal of Medicinal Chemistry

Article

Design and Synthesis of Orally Bioavailable 4-Methyl Heteroaryldihydropyrimidine Based Hepatitis B Virus (HBV) Capsid Inhibitors

Zongxing Qiu, Xianfeng Lin, Mingwei Zhou, Yongfu Liu, Wei Zhu, Wenming Chen, Weixing Zhang, Lei Guo, Haixia Liu, Guolong Wu, Mengwei Huang, Min Jiang, Zhiheng Xu, Zheng (Joe) Zhou, Ning Qin, Shuang Ren, Hongxia Qiu, Sheng Zhong, Yuxia Zhang, Yi Zhang, Xiaoyue Wu, Liping Shi, Fang Shen, Yi Mao, Xue Zhou, Wengang Yang, Jim Zhen Wu, Guang Yang, Alexander V Mayweg, Hong C Shen, and Guozhi Tang

J. Med. Chem., **Just Accepted Manuscript** • DOI: 10.1021/acs.jmedchem.6b00879 • Publication Date (Web): 26 Jul 2016

Just Accepted

ACS Publications

Journal of Medicinal Chemistry is published by the American Chemical Society. 1155 Sixteenth Street N.W., Washington, DC 20036

	Shen, Hong; Roche R&D Center China, Medicinal chemistry Tang, Guozhi; Roche Pharma Research and Early Development,

Design and Synthesis of Orally Bioavailable 4-Methyl Heteroaryldihydropyrimidine Based Hepatitis B Virus (HBV) Capsid Inhibitors

Zongxing Qiu,[‡,‡] Xianfeng Lin,[‡,‡] Mingwei Zhou,[‡,‡] Yongfu Liu,[‡,‡] Wei Zhu,[‡,‡] Wenming Chen,[‡,‡] Weixing Zhang,[‡,‡] Lei Guo,[‡,‡] Haixia Liu,[‡,‡] Guolong Wu,[‡,‡] Mengwei Huang,[‡,‡] Min Jiang,[‡,‡] Zhiheng Xu,[‡,†] Zheng Zhou,[‡,†] Ning Qin,[‡,†] Shuang Ren,[‡,∥] Hongxia Qiu,[‡,∥] Sheng Zhong,[‡,∥] Yuxia Zhang,[‡,∥] Yi Zhang,[‡,∥] Xiaoyue Wu,[‡,∥] Liping Shi,[‡,§] Fang Shen,[‡,§] Yi Mao,[‡,§] Xue Zhou, [‡,§] Wengang Yang,[‡,§] Jim Z. Wu,[‡,§] Guang Yang,[‡,§] Alexander V. Mayweg,[‡,‡] Hong C. Shen,[‡,‡] and Guozhi Tang [‡,‡,*]

[‡]*Roche Pharma Research and Early Development, Roche Innovation Center Shanghai,* [‡]*Medicinal Chemistry,* [†]*Chemical Biology,* [∥]*Pharmaceutical Sciences,* [§]*Discovery Virology, 720 Cailun Road, Shanghai, 201203 China*

ABSTRACT—Targeting the capsid protein of hepatitis B virus (HBV) and thus interrupting normal capsid formation has been an attractive approach to block the replication of HBV viruses. We carried out multidimensional structural optimizations based on the heteroaryldihydropyrimidine (HAP) analogue Bay41-4109 (**1**) and identified a novel series of HBV capsid inhibitors that demonstrated promising cellular selectivity indexes, metabolic stabilities, and in vitro safety profiles. Herein we disclose the design, synthesis, structure−activity relationship (SAR), co-crystal structure in complex with HBV capsid proteins, and in vivo pharmacological study of the 4-methyl HAP analogues. In

* Tel.: +86 21 28946723. Fax: +86 21 50790292. E-mail: gordon.tang@roche.com

particular, the (2*S*, 4*S*)-4,4-difluoroproline substituted analogue **34a** demonstrated high oral bioavailability and liver exposure, and achieved over 2-log viral load reduction in a hydrodynamic injected (HDI) HBV mouse model.

Keywords— hepatitis B virus (HBV), capsid inhibitor, heteroaryldihydropyrimidine, capsid assembly

INTRODUCTION

Chronic hepatitis B virus (HBV) infection remains a major threat to public health despite the fact that HBV vaccination programs have been extensively implemented in the past. There are about 350 million chronic HBV carriers in the world and disease progression among many of them often leads to cirrhosis and hepatocellular carcinoma.[1] It has been estimated that HBV infection directly or indirectly accounts for an annual death of 600,000 patients. Nevertheless, current treatment options are limited to interferons (IFNs) and nucleos(t)ides-based reverse transcriptase inhibitors that do not offer a satisfactory clinical cure rate for chronic HBV carriers.[2] For example, the response rate in HBeAg-positive patients following 4-5 years of treatment with nucleos(t)ides is about 0-10%, and 8-15% with pegylated IFN-α or pegylated IFN-α plus lamivudine, whereas the response rate in HBeAg-negative patients is even lower. Of note, nucleos(t)ide therapies typically require lifetime treatment to prevent viral rebound while IFNs require parenteral administration and are associated with adverse effects such as 'flu-like' symptoms. To achieve a higher HBV cure rate than current standard of care, a multipronged approach with new molecular entities is very likely required.[3, 4] As such, there is a tremendous unmet medical need to identify and develop novel, efficacious and safe anti-HBV agents with diverse mechanisms of action.

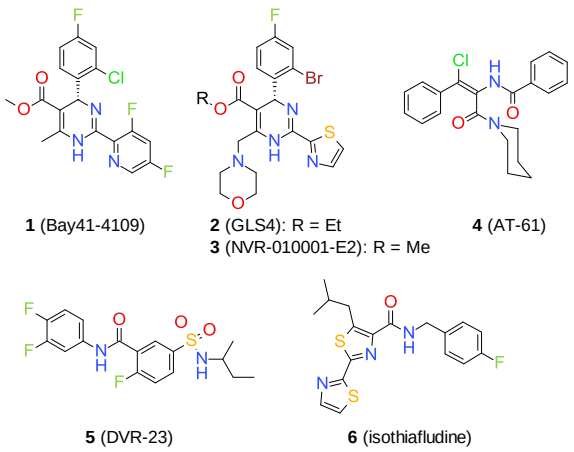

Figure 1. Chemical structures of reported HBV capsid inhibitors.

As a structural component of the viral nucleocapsid, the HBV capsid protein plays multiple roles in the HBV lifecycle including reverse transcription of pre-genomic RNA (pgRNA), formation and intracellular trafficking of relaxed circular-DNA, and subviral particle formation.[5, 6] To date a number of reported capsid inhibitors (or effectors) are able to interrupt normal capsid assembly and thus inhibit HBV DNA synthesis (Figure 1). Among them, Bay 41-4109 (**1**), a heteroaryldihydropyrimidine (HAP) compound, is a seminal HBV capsid inhibitor that has been well studied in the past.[7] Mechanistic and biostructural studies indicate that **1** can fit into a hydrophobic pocket located at the interface of capsid dimers and trigger aberrant capsid assembly and aggregation.[8] Treatment of virus-producing HepG2.2.15 cells with **1** leads to reduction of HBV DNA as well as dose-dependent depletion of core proteins and nucleocapsids.[7] However, further development of **1** has been hindered by several factors including in vitro and in vivo toxicity and limited efficacy in animal models.[9, 10] GLS-4 (**2**) and **3** are a new generation of HAP analogues featuring 6-morpholine substituents and 2-thioazolyl groups attached to the core scaffold.[11–13] Although reported to be more potent and less cytotoxic in in vitro tests, **2** demonstrated similar in vivo effects as **1** in a mouse model.[11] Acrylamide **4** (previously reported as AT-61 but with the wrong *E*-configuration),[14, 15] sulfamoylbenzamide **DVR23** (**5**),[16] and isothiafludine (**6**)[17] are the other class of capsid inhibitors that

have distinct effects on the HBV capsid assembly process from that of HAPs. Mechanistically, compounds **4**–**6** also bind to capsid proteins and accelerate the capsid assembly process, but they usually result in normal-sized and pgRNA-free empty capsids. Sometimes referred to as pgRNA encapsidation blockers, **4**–**6** inhibit HBV DNA synthesis without the capsid depletion effects of HAPs.[16–18] Whether the in-cell capsid depletion induced by HAPs provides an extra benefit to treat HBV infection or not remains to be investigated in relevant animal models and eventually in a clinical setting.

To develop novel, orally bioavailable and in vivo efficacious anti-HBV agents, we attempted to explore the chemistry space of HAPs from benchmark analogue **1** with goals to enhance anti-HBV activity, reduce cytotoxicity, and improve metabolic stability and in vitro safety profiles.

RESULTS AND DISCUSSION

Section 1. Design and Synthesis of 4-Methyl HAPs. Because of the lack of high resolution co-crystal structures of capsid protein and HAPs at the time,[8] an information-driven approach was carried out to optimize the HAP series represented by **1**. Firstly, metabolite identification studies of **1** upon incubation with human and mouse liver microsomes (HLM and MLM) indicated that aromatization of the dihydropyrimidine core (M-2H) is a major metabolic pathway. When evaluated in HepDE19 cells that support high levels of HBV DNA replication,[19] **1** demonstrates anti-HBV activity with an EC_{50} of 0.14 μM. The corresponding CC_{50} value of **1** is 13.4 μM in the same cell line. Further structure-activity relationship (SAR) study of 4-H HAPs revealed that 2-Cl on the 4-phenyl head group is indispensable to their anti-HBV activities and that the 3,5-difluoropyridinyl moiety is chemically susceptible to nucleophilic S_NAr displacements (unpublished results). Taken together, it was anticipated that 4-methyl-substituted HAPs would not be susceptible to aromatization, and that the methyl group could also take a position close to the 2-Cl substituent of **1** and recapitulate its role in capsid binding (Figure 2). Indeed, predicted lowest energy conformations of 4-methyl HAP **7a** (4-*S*

enantiomer as shown) and 4-H HAPs like **1** overlay well with one another and the 4-methyl group of **7a** points in the same direction as the 2-Cl substituent of **1**. Further conformation analysis also suggested that the 4-phenyl group of **7a** remains orthogonal to the HAP core and that the 2-thiazolyl moiety is essentially co-planar with the HAP core due to the formation of an intramolecular hydrogen bond and 1,4-N−S interaction.[20] Thus, a series of 4-methyl-substituted HAP analogues including **7a**−**c** were synthesized and evaluated in HepDE19 cells.

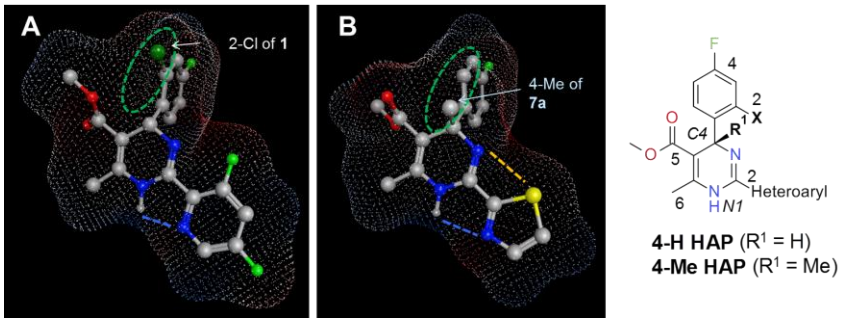

Figure 2. Predicted lowest energy conformations of **1** (A) and (*S*)-enantiomer of **7a** (B) in vacuum. Force field MMFF94x[21] was applied in Molecular Operating Environment (MOE), CCG. An intramolecular hydrogen-bonding (HB) interaction between 1-NH and 2-heteroaryl group is indicated. Molecules are presented as ball and stick with electrostatic surface included. Carbon, oxygen, nitrogen, fluorine and chlorine atoms are shown in gray, red, blue, green and dark green colors, respectively.

Generally, 4-methyl HAP analogues can be prepared from β-ketoester **8** and a variety of benzaldehydes **9** according to the procedures shown in Scheme 1. Briefly, an aldol condensation of **8** and **9** was carried out and the resulting products were treated with CH_3CuLi to give 1,4-Michael addition products **10**. Ketoesters **10** were then treated by a two-step phenylselenation and oxidation to give α, β-unsaturated esters **11**, which were separated and used in the subsequent step as a mixture of E/Z-isomers. The condensation and ring cyclization reactions of **11** and amidines **12** turned out quite sluggish and complicated, in part because of high steric hindrance and decomposition of **11** at high temperature. To minimize the decomposition issue, olefins **11** were dissolved in NMP and added dropwise into a stirring mixture of **12** and $NaHCO_3$ in NMP that was pre-warmed to 120 ℃. By this

method, the methyl-substituted HAP scaffold with a quaternary carbon was successfully built up from **11** and **12** in moderate to high yields.

Scheme 1. Synthesis of 4-Alkyl-substituted HAP Analogues **7a–j**[a]

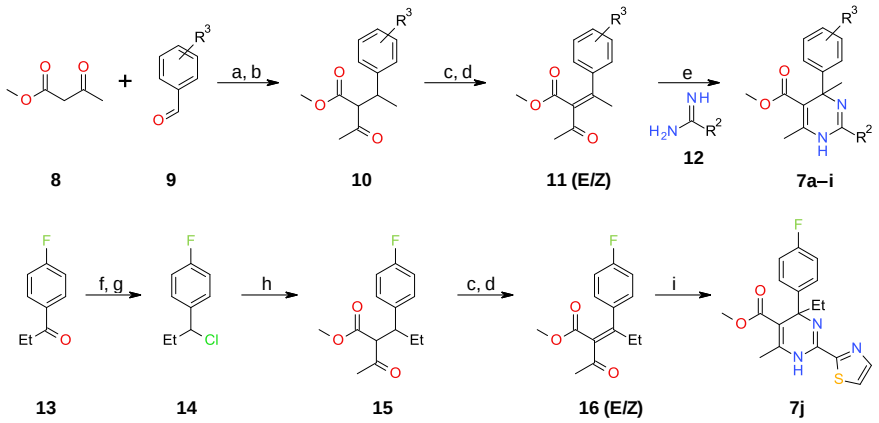

[a] Reagents and conditions: (a) piperidine, HOAc, EtOH; (b) CH_3CuLi, THF, −78 ℃; (c) PhSeCl, NaH, THF; (d) H_2O_2/H_2O, DCM; (e) $NaHCO_3$, NMP, 120 ℃, 2 h, 30−70%; (f) $NaBH_4$, EtOH; (g) $SOCl_2$, DCM, 90% for 2 steps; (h) **8**, NaH, THF, 60%; (i) thiazole-2-carboxamidine, AcOK, *i*-PrOH, 120 ℃, 15%.

Section 2. SAR at the 4-Phenyl Head Group of 4-Methyl HAPs. Analogues **7a** and **7b** moderately reduced HBV DNA in cellular activity tests with EC_{50} values of 11.6 μM and 7.1 μM, respectively (Table 1). On the other hand, they were also much less cytotoxic to HepDE19 cells with CC_{50} values above 100 μM and had good aqueous solubility in lyophilized solubility assays (LYSA). To confirm the anti-HBV activity of this new HAP scaffold, we conducted chiral separation of **7a** by supercritical fluid chromatography (SFC) and determined that enantiomer (*S*)-**7a** is active in HepDE19 cells with an EC_{50} of 6.8 μM. The absolute configuration of (*S*)-**7a** was confirmed by single crystal X-ray studies, and it is clear that the core structures and 4-phenyl head groups of (*S*)-**7a** and **1** are well aligned to each other (see the Supporting Information). Notably, analogue **7c** with the same 2-Cl, 4-F phenyl group of **1** was less active than **7a** and **7b** and was more cytotoxic to HepDE19 cells with a CC_{50} of 82.5 μM. The 2-Cl substituent of **7c** may occupy a position opposite to the 4-methyl group, an

orientation that may not favor target binding. Furthermore, 4-methyl HAPs may generally have different SAR and chemistry space relative to **1**, especially at the 4-phenyl head group. Thus, additional structural explorations of the 4-methyl HAPs were carried out in an attempt to rescue their in vitro anti-HBV activities.

Table 1. The Effects on HBV DNA Reduction and Physicochemical Properties of **7a–j**

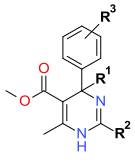

7a–j

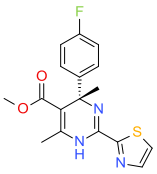

(*S*)-**7a**

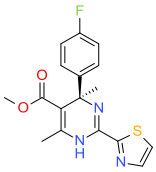

(*R*)-**7a**

ID	R^1	R^2	R^3	EC_{50}[a]	CC_{50}[b]	SI[c]	logP[d]	LYSA[e]
1	H		2-Cl, 4-F	0.14	13.4	96	4.6	38
7a	Me		4-F	11.6	>100	>9	4.2	22
(*S*)-**7a**	Me		4-F	6.8	>100	>15	4.2	ND
7b	Me		4-F	7.1	>100	>14	4.4	178
7c	Me		2-Cl, 4-F	28.1	82.5	3	4.8	18
7d	Me		H	35.9	>100	>3	4.0	ND
7e	Me		4-Cl	26.8	43.6	2	4.6	14
7f	Me		4-SO_2Me	>100	>100	-	2.5	365
7g	Me		4-OMe	>100	>100	-	4.0	106
7h	Me		4-CN	>100	>100	-	3.5	87
7i	Me		3-F, 4-F	4.1	85.9	21	4.4	50
7j	Et		4-F	>100	96.0	-	4.6	ND

[a]EC_{50} values [μM] for the reduction of HBV DNA in HepDE19 cells. The levels of HBV DNA in supernatant were determined by dot-blot experiments in duplicate runs, with variation < 15%.

[b]CC_{50} values [μM] measured by CCK-8 in HepDE19 cells. Experiments were in duplicate runs with variation < 15%.

[c]Selectivity index (SI) of CC_{50}/EC_{50} in HepDE19 cells.

[d]Predicted partition coefficient between octanol phase and water phase (K_{ow}logP).

[e]Lyophilized solubility assay (LYSA) from duplicate runs, mean values reported in μg/mL with variation < 10%).

A number of analogues with structure variations at the 4-phenyl head group (substitution at the C4 of the HAP core) were prepared and evaluated for their anti-HBV activities (Table 1). SAR analysis indicated that the *p*-F substituent on the 4-phenyl group is critical for anti-HBV activity and that replacements like −H, $-SO_2Me$, −OMe and −CN reduce potency in HepDE19 cells (analogues including **7d** and **7f**−**h**). Just like **7c**, analogue **7e** had inferior cytotoxicity and metabolic stability profiles with MLM of 85 mL min^{-1} kg^{-1}, presumably due to their high lipophilicity (K_{ow}logP ≥ 4.6). On the other hand, polar and electron-withdrawing substituents such as $-SO_2Me$, −CN, $-CO_2H$ and amide groups improved the metabolic stability and solubility profiles of 4-methyl HAPs. For example, analogues **7f** and **7h** showed lower intrinsic clearance with MLM of 57 and 75 mL min^{-1} kg^{-1}, respectively. Introducing a second fluorine substitution at the *m*-position improved the potency of analogue **7i** relative to **7a,** with an EC_{50} of 4.1 μM. However, **7i** was also highly lipophilic (KowlogP = 4.4) with MLM of 83 mL min^{-1} kg^{-1}. We speculated that the head groups sit in a hydrophobic pocket making close molecular contacts with HBV capsid proteins such that minor structural modifications can have profound effects on anti-HBV activity.

Considering the SAR findings discussed above, we explored the tolerability of larger alkyl groups including ethyl at the 4-position of HAPs. To synthesize the 4-ethyl-substituted HAP analogue **7j**, ketone **13** was reduced with $NaBH_4$ and the resulting alcohol was converted to substituted benzyl chloride **14** (Scheme 1). Chloride **14** was then treated with **8** and NaH to afford β-ketoester **15**. By using the same methods as described previously, tetra-substituted olefin **16** was obtained and it was added into a mixture of thiazole-2-carboxamidine and KOAc in isopropanol at 120 ℃ to give analogue

7j. Unforutnately, **7j** was inactive in HepDE19 cells (Table 1). Thus the 4-methyl HAP core was fixed in subsequent explorations of structure-property relationships focused on the 2-heteroaryl and 5-, 6-positions of the HAP core.

Section 3. SAR of 2-Heteroaryls in 6-Morpholine-substituted 4-Methyl HAPs. As in the case of 4-H HAPs like **2** and **3**,[11, 22] a solubilizing 6-morpholine substituent may help improve in vitro anti-HBV potency yet its impact on the 4-methyl HAPs remained to be investigated. Accordingly, 6-morpholine substituted analogues **18a**−**k** were prepared from racemic or optically pure intermediates **7** (Scheme 2). As an efficient method, 4-methyl HAPs were treated with $(Boc)_2O$ anhydride and *N*, *N'*-dimethylaminopyridine (DMAP) and the *N*-Boc protected products were treated with NBS and azobisisobutyronitrile (AIBN) at 50 ℃ to give bromides **17**. Without purification, bromides **17** were substituted with morpholine and the products were treated with trifluoroacetic acid (TFA) to give analogues **18a**−**k** in over 40% yields.

Generally, the 6-morpholine substituted 4-methyl HAPs demonstrated better cellular activities than their parent compounds in HepDE19 cells. For example, enantiomer (*S*)-**18a** was 40 times more active than (*S*)-**7a** with an EC_{50} of 0.17 μM (Table 2). 3,4-Difluoro-substituted analogue (*S*)-**18b** significantly reduced HBV DNA with an EC_{50} of 70 nM in HepDE19 cells. However, 3-Cl, 4-F-substituted analogue **18c** was over 100 times less active than (*S*)-**18b** with an EC_{50} of 8.1 μM and a CC_{50} of 67.7 μM. In agreement with previous SAR observations, enantiomers (*R*)-**18a** and (*R*)-**18b** had moderate to weak anti-HBV activities with EC_{50} values of 26.8 μM and 65.8 μM, respectively.

Scheme 2. Synthesis of 4-Methyl HAP Analogues **18a**−**k**[a]

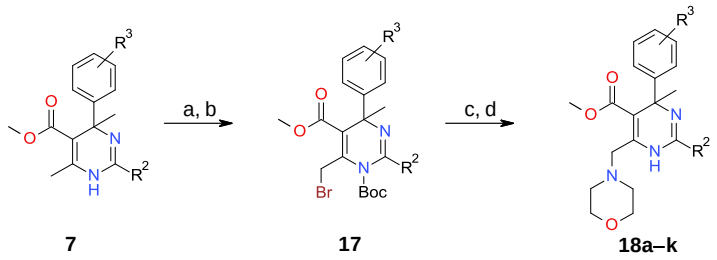

[a] Reagents and conditions: (a) $(Boc)_2O$, DMAP, DCM, rt, overnight; (b) NBS, AIBN, CCl_4, 50 ℃, 2 h; (c) morpholine, DCM, 50 ℃, 1 h; (d) TFA, DCM, rt.

(*S*)-**18a** and (*S*)-**18b** are highly potent anti-HBV inhibitors with selectivity margins in HepDE19 cells that meet our primary goals for in vitro potency. However, they have poor metabolic stability and limited oral availability. For example, the mouse liver microsome (MLM) clearance of (*S*)-**18a** and (*S*)-**18b** was 81 and 89 mL min^{-1} kg^{-1}, respectively. The oral bioavailability (*F*) of (*S*)-**18a** was about 1.5% in a mouse single dose pharmacokinetics (SDPK) study. We therefore set out to improve the metabolic stability of HAPs and to identify orally bioavailable analogues with sufficient target organ exposure for in vivo efficacy studies.

In an attempt to improve microsomal stability and physiochemical properties, the 2-thiazolyl group was replaced with polar heteroaryls to reduce lipophilicity, and analogues such as **18d**−**j** were prepared accordingly. A number of these analogues had increased microsomal stability relative to (*S*)-**18a** and also were expected to have good aqueous solubility based on LYSA results of > 300 μg/mL (Table 2). Both *N*-methyl imidazolyl and 5-F pyridinyl groups were tolerated with EC_{50} values < 1 μM (analogues **18d** and **18f**), whereas oxazolyl (**18e**), pyrimidinyl (**18i**) and pyridazinyl (**18j**) resulted in lower potencies than (*S*)-**18a**. Our results also suggested that polar substituents cannot be tolerated on the heteroaryls, for example, 5-methoxypyridinyl analogue **8g** was 25 times less active than **18f**. In addition, aliphatic groups were not tolerated at the 2-position of HAPs, leading to a total loss of activity (analogue **18k**).

Table 2. The Effects on HBV DNA Reduction and Physicochemical Properties of **18a**−**k**

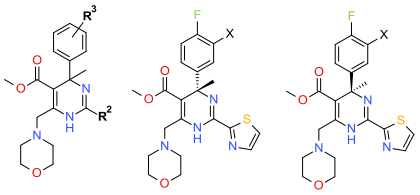

18a–k (*S*)-**18a** (X = H) (*S*)-**18b** (X= F) (*R*)-**18a** (X = H) (*R*)-**18b** (X = F)

ID	R^2	R^3	EC_{50}[a] [μM]	CC_{50}[a] [μM]	SI	logP	LYSA[a] [μg/mL]
(*S*)-**18a**		4-F	0.17	>100	>588	3.0	14
(*R*)-**18a**		4-F	26.8	>100	>4	3.0	16
(*S*)-**18b**		3-F, 4-F	0.07	>100	>1429	3.2	7
(*R*)-**18b**		3-F, 4-F	65.8	>100	-	3.2	ND
18c		3-Cl, 4-F	8.1	67.7	8	3.6	3
18d		4-F	0.65	>100	>154	2.6	435
18e		4-F	10.1	>100	>10	2.7	336
18f		4-F	0.61	>100	>164	3.0	2
18g		4-F	3.65	> 100	> 27	3.3	22
18h		4-F	15.6	>100	>6	2.9	77
18i		4-F	2.95	>100	>34	1.9	424
18j		4-F	3.65	>100	>27	2.5	341
18k		4-F	>100	>100	-	3.0	ND

[a] Definitions are the same as those described in Table 1.

Section 4. SAR at 5-position of 4-Methyl HAPs. The 5-ester group appeared to have unclear roles in target binding. In our SAR studies of the 5-ester group, we found that direct chemistry conversions of the ester moiety were problematic. Neither hydrolysis nor reduction of analogues like **7** gave desired products even under harsh conditions, probably due to conjugation effects with the HAP core and high steric hindrance of the ester moiety. To address these issues, *t*-butyl β-ketoester **19** was used as the starting material and *t*-butyl ester **20** was prepared by means of the same method as shown in Scheme 1. Treatment of **20** with TFA smoothly afforded acid **21** and further functionalization was in

turn carried out (Scheme 3). In one case, **21** was treated with 2-(7-aza-1H-benzotriazole-1-yl)-1,1,3,3-tetramethyluronium hexafluorophosphate (HATU) and ammonia to give primary amide **22**, which was then converted to 5-CN analogue **23** upon treatment with trifluoroacetic acid anhydride (TFAA). On the other hand, amide analogues such as **24** and **25** were prepared by treating **21** with *N*, *N'*-carbonyldiimidazole (CDI) and then specified amines at elevated temperature. Amide **25** was treated with polyphosphoric acid (PPA) at 120 ℃ to give 5-oxazole-substituted analogue **26**. Finally, analogues **27a**−**e** were prepared by converting their respective precursors to bromide intermediates and then subsequently treating with morpholine. Besides exploring the polarity and heteroaryl vectors like oxazole, we also looked into steric factors via isopropyl ester **27f**, which was synthesized with isopropyl β-ketoester as the initial starting material.

Scheme 3. Synthesis of HAP Analogue **27a**−**e**[a]

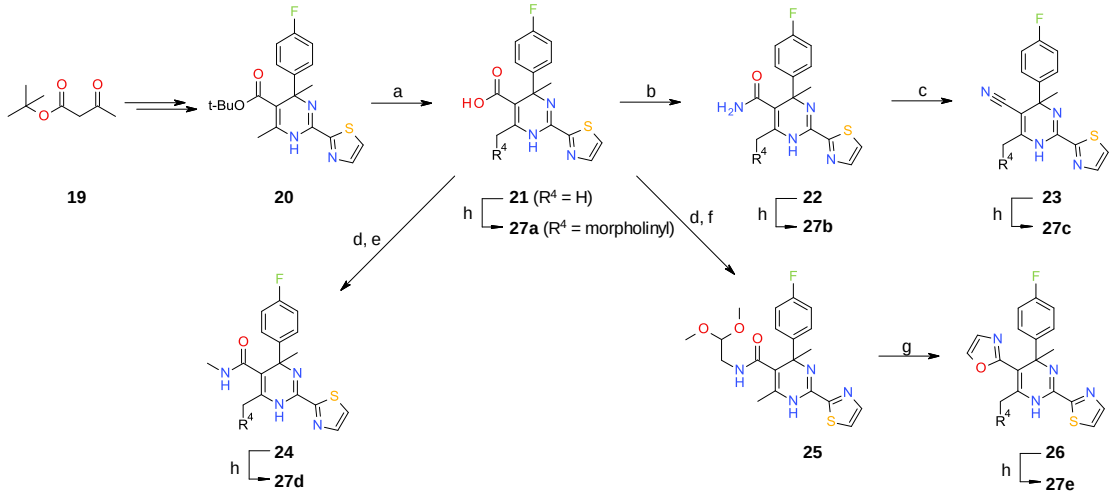

[a] Reagents and conditions: (a) TFA, DCM, 3 h, 100%; (b) HATU, NH_3, NEt_3, DCM, 40%; (c) TFAA, DCM, 3 h, 87%; (d) CDI, THF; (e) $CH_3NH_2{\cdot}HCl$, NEt_3, CH_3CN, 90 ℃, 80%; (f) 2,2-dimethoxyethanamine, CH_3CN, 0.5 h, 120 ℃, MW, 90%; (g) PPA, 2 h, 120 ℃, 30%; (h) NBS, AIBN, CCl_4, 50 ℃, 2 h then morpholine, DCM, 50 ℃, 1 h, >20% over 2 steps.

The cellular activities, physicochemical properties and microsome stabilities of analogues **27a**−**f** are shown in Table 3. Polar groups such as $-CO_2H$ and amides improved microsome stability as

well as solubility but were not tolerated with EC_{50} values > 100 μM in HepDE19 cells (analogues **27a/b/d**). Heteroaryls and bulky groups like isopropyl ester were also detrimental to both cellular potency and metabolic stability. For example, analogues **27e** and **27f** showed moderate anti-HBV activities and narrow selectivity margins, with reduced metabolic stabilities in liver microsomes. In contrast, the less lipophilic 5-CN analogue **27c** had a better selectivity margin and microsome stability than **27e** and **27f**, with an EC_{50} of 2.7 μM in HepDE19 cells.

Table 3. The Effects on HBV DNA Reduction and Physicochemical Properties of **27a–f**

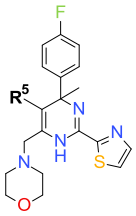

27a-f

ID	R^5	EC_{50}[a] [μM]	CC_{50}[a] [μM]	SI[a]	logP[a]	LYSA[a] [μg/mL]	MLM[b]
27a	$-CO_2H$	>100	>100	-	1.0	>504	6
27b		61.8	>100	-	1.9	515	59
27c	−CN	2.7	>100	>37	2.4	6	79
27d		>100	>100	-	1.9	573	77
27e		2.0	42.3	21	3.4	263	89
27f		6.1	74.7	12.2	3.9	1	88

[a]Definitions are the same as those described in Table 1.

[b]Scaled intrinsic clearance [mL min^{-1} kg^{-1}] in mouse liver microsome (MLM). Experiments were run in duplicate, with variation < 10%.

Section 5. SAR at the 6-position of 4-Methyl HAPs. As part of our effort to optimize the 4-methyl HAP series, we sought to address the potential metabolic liability of the 6-morpholine moiety

that is often associated with N−C and O−C cleavage. Thus, we developed a highly efficient and easily scalable synthesis of **7a**. First, tetrasubstituted olefin **29** was obtained by one-step indium (III)-catalyzed condensation of β-ketoester **8** and alkyne **28** in 40% yield (Scheme 4).[23] Second, the condensation of **29** and thiazole-2-carboxamidine was carried out as described before and the product **7a** was converted to bromide intermediate **30** for chemical diversification. Finally, in the case of *N*-linked analogues, **30** was treated with selected amines or (sulfon)amides (**32**) and complementary bases such as K_2CO_3 and *t*-BuOK in DMF. The resulting products were then treated with TFA to give **31a**−**r** (Table 4). For the synthesis of 6-amino acid substituted analogues **31s**−**t**, amino esters were alkylated with bromide **30**, followed by LiOH-mediated hydrolysis and finally removal of the *N*-Boc protecting group. These analogues were then tested in HepDE19 cells.

Scheme 4. Synthesis of *N*-linked and *O*-linked Analogues **31a**−**w**[a]

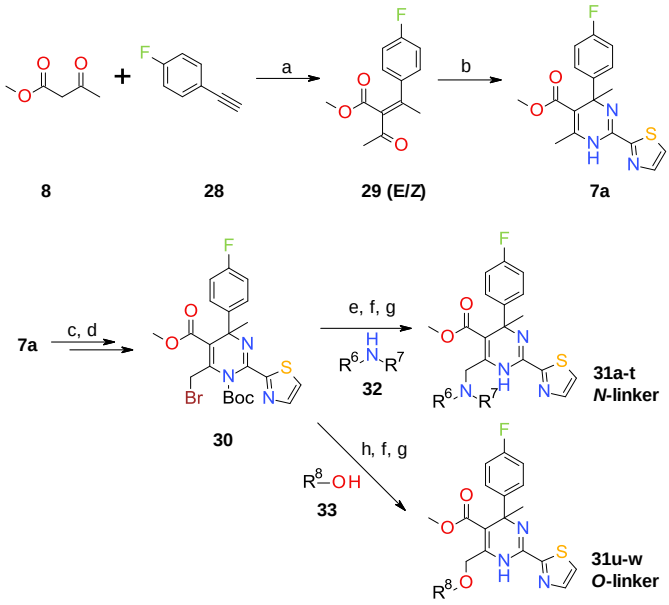

[a] Reagents and conditions: (a) $In(OTf)_3$, o-xylene, 120 ℃, 1 h, 40%; (b) thiazole-2-carboxamidine, $NaHCO_3$, NMP, 120 ℃, 2 h, 60%; (c) $(Boc)_2O$, DMAP, DCM, rt, overnight; (d) NBS, CCl_4, 50 ℃, 2 h, 82% for 2 steps; (e) amine **32**, K_2CO_3 or *t*-BuOK [for (sulfon)amides], DMF, 40 ℃, 3 h; (f) LiOH, MeOH/H_2O, rt, 2h for hydrolysis of the amino ester group; (g) TFA, DCM, rt, 2 h; (h) alcohol **33**, NaH, THF, rt, overnight.

Substitution of the morpholine group with piperidine and piperazine, common "bioisosteres" of morpholine, led to a complete loss of activity (analogues **31a**–**b**). *Gem*-dimethyl morpholine was well tolerated (**31c**), suggesting that some steric bulk could be accommodated. However, a conformationally-constrained bridged morpholine led to a significant potency drop (**31d**). Finally, lactams were clearly detrimental and both **31e** and **31f** had weak cellular activities.

Without knowing the molecular interactions that the morpholine group plays in capsid binding, we attempted to identify fragments that may resemble the role of the morpholine oxygen atom. The 4-hydroxyl piperidine analogue **31g** was weakly active with an EC_{50} of 65.2 μM, while analogues with thiomorpholine dioxide and 4,4-difluoro piperidine substitutions (**31h** and **31i**) were about 10 times more potent than **31g**. By shifting the *gem*-difluoro substituents to the 3-position of the piperidine ring, the anti-HBV potency was further improved as analogue **31j** had an EC_{50} of 2.1 μM. Next, 3,3-difluoropyrrolidine-substituted analogue **31m** was prepared and showed a 15-fold improvement over **31j** with an EC_{50} value of 0.14 μM. In contrast, 3-CF_3-substituted pyrrolidine analogue **31n** had moderate potency with an EC_{50} of 8.1 μM and 3-hydroxyl pyrrolidine analogue **31k** was only weakly active. Notably, sulfonamide analogue **31p** had better activities than lactams **31e** and **31f**, and groups like imidazole and azetidine were not tolerated (analogues **31q**–**r**).

Table 4. The Effects on HBV DNA Reduction and Physicochemical Properties of **31a**–**w**

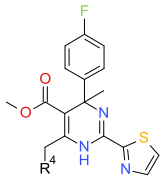

31a-w

ID	R^4	EC_{50}[a] [μM]	CC_{50}[a] μM]	SI	logP	LYSA[a] [μg/mL]	MLM[a] [mL min^{-1} kg^{-1}]
31a		>100	>100	-	4.7	282	88
31b		>100	>100	-	2.7	250	39

31c		0.19	66.6	350	3.4	13	88
31d		17.3	>100	>6	3.2	564	84
31e		65.3	>100	-	2.4	440	80
31f		70.2	>100	-	2.1	34	81
31g		65.2	>100	-	3.2	593	81
31h		6.4	>100	>16	1.8	15	66
31i		7.1	>100	>14	4.5	< 1	88
31j		2.1	>100	>48	4.5	ND	89
31k		64.7	>100	-	2.7	503	83
31m		0.14	92	657	4.0	5	89
31n		8.1	46	6	5.1	13	88
31p		16.7	>100	>6	3.3	125	79
31q		>100	>100	-	3.9	338	69
31r		>100	>100	-	2.9	ND	88
31s		>100	>100	-	0.6	ND	ND
31t		21.3	>100	>5	1.3	>510	42
31u		8.1	>100	>12	3.4	30	79
31v		6.4	98	15	4.3	19	81
31w		24.4	>100	>4	3.5	>649	24

[a] Definitions are the same as those described in Table 1.

In addition, structural explorations with noncyclic amines were carried out. Among those modifications, the α-aminocyclopropanecarboxylic acid substituted analogue **31t** demonstrated

moderate cellular potency with an EC_{50} of 21.3 μM. In particular, **31t** had significantly improved solubility and metabolic stability compared to other analogues with LYSA > 510 μg/mL and MLM of 42 mL min^{-1} kg^{-1}, respectively. It seems that the *c*-Pr moiety is important for cellular activity as sarcosine substituted analogue **31s** was inactive. Subsequently, we applied the SAR learning from the *N*-linked series and prepared *O*-linked analogues by treating bromide **30** with alcohols **33** and NaH, followed by the removal of the *N*-Boc protecting group by TFA (Scheme 4). **31u**−**w** had moderate anti-HBV activities, and carboxylic acid analogue **31w** had highly attractive physicochemical properties with LYSA > 649 μg/mL and MLM of 24 mL min^{-1} kg^{-1} (Table 4).

Scheme 5. Design and Synthesis of Amino Acid Substituted HAPs **34a**−**f**[a]

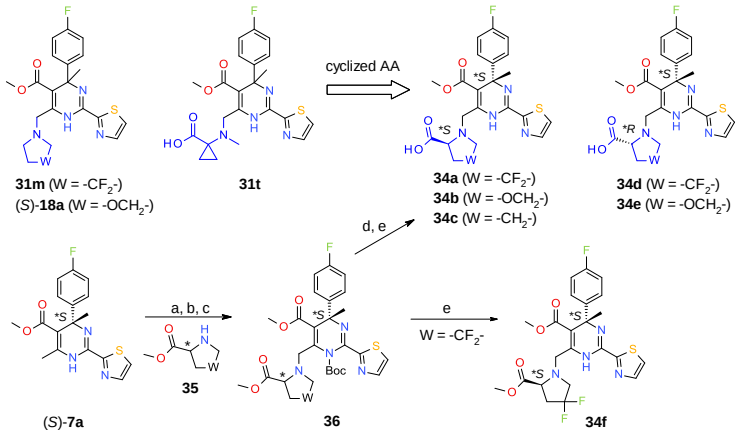

[a] Reagents and conditions: (a) $(Boc)_2O$, DMAP, DCM, rt, overnight; (b) NBS, CCl_4, 50 ℃, 2 h, 82% for 2 steps; (c) amino ester, K_2CO_3, DMF, 40 ℃, 3 h; (d) LiOH, MeOH, rt, 2h; (e) TFA, DCM, rt, 2 h.

Section 6. Design of 6-Cyclic Amino Acid Substituted 4-Methyl HAPs. Analogues **31c** and **31m** were highly potent in vitro but lacked sufficient systemic exposure for in vivo efficacy studies, because of their lipophilic characteristics. A logical next step was to combine their 6-substituents with that of carboxylic acid-based analogues **31t** and **31w**, which had moderate activities but nevertheless promising physicochemical properties. Thus, the 6-cyclic amino acid substituted analogues **34a**−**e** were synthesized from optically pure intermediate (*S*)-**7a** according to the procedures shown in Scheme 5.

Esters **36** were obtained in medium to high yields after *N*-Boc protection of (*S*)-**7a**, bromination and subsequent S_N2 reaction with chiral amino esters **35**. Esters **36** were then hydrolyzed with LiOH and the resulting acid intermediates were treated with TFA to give desired products.

Among them, the (2*S*, 4*S*)-4,4-difluoroproline substituted analogue **34a** demonstrated significantly improved potency and solubility profiles with an EC_{50} of 0.084 μM and LYSA > 645 μg/mL (Table 5). Importantly, **34a** had a selectivity index (SI) of 1905-fold in HepDE19 cells, a significant improvement over **1**. The (2*R*, 4*S*)-4,4-difluoroproline substituted analogue **34c** was significantly less active than its diastereoisomer **34a** with an EC_{50} of 6.6 μM, as was the (2*R*, 4*S*)-morpholine acid analogue **34d** in comparison to diastereoisomer **34b**. Interestingly, the (2*R*, 4*S*)-isomers had better stability profiles than the corresponding (2*S*, 4*S*)-isomers in both human and mouse liver microsome stability tests (analogues **34a**–**d**). The *gem*-difluoro substituents and the carboxylic acid moiety appear to be important for anti-HBV activity since the (2*S*, 4*S*)-proline analogue **34e** lost activity and the ester analogue **34f** was a few times less active than **34a**.

Table 5. The Effects on HBV DNA Reduction and Physicochemical Properties of 6-Amino Acid Derivatives **34a**–**f**

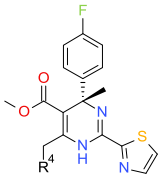

34a-f

ID	R^4	EC_{50}[a] [μM]	CC_{50}[a] [μM]	SI[a]	logP[a]	LYSA[a] [μg/mL]	MLM[a] [mL min^{-1} kg^{-1}]	HLM[a] [mL min^{-1} kg^{-1}]
34a	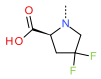	0.084	160	1905	1.2	>645	84	12
34b		0.77	>100	>357	0.14	>633	80	4.1
34c	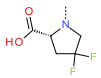	6.6	82.3	12	1.2	>659	60	0

34d		3.0	>100	>15	0.14	>633	61	0
34e		>100	>100	-	1.4	>589	14	2.3
34f		0.66	>100	>151	3.5	ND	90	23

[a] Definitions are the same as those described before. HLM, human liver microsomal test.

Section 7. Co-crystal Structure of 34a in Complex with HBV Capsid Protein. To gain additional SAR understanding and elucidate the molecular interaction network of 4-methyl HAPs with the HBV capsid protein, we carried out crystallization studies with those amino acid-based analogues. A high resolution co-crystal structure of **34a** in complex with Y132A mutant capsid protein was obtained with diffraction up to 1.7Å (PDB 5GMZ). The 4-methyl HAP scaffold of **34a** fits into the hydrophobic pocket of the capsid protein dimer-dimer interface consistent with the 5Å-complex structure of HAP1, a close analogue of **1**.[8, 22] It is clear that the 2-thiazolyl group of **34a** is co-planar with the dihydropyrimidine core as anticipated and is buried in a well-defined hydrophobic cavity formed by residues Phe23, Pro25, Tyr118, Trp102, Thr128' and Ala132' (Figure 3). In addition, 4-methyl substitution on the core and the *p*-fluorophenyl group of **34a** occupy an adjacent and larger hydrophobic pocket and make van der Waals (VDW) contacts with residues including Pro25, Leu30, Thr33, Trp102, Ile105, Ser106, Val124', Arg127', and Thr128'. Given the limited space around the *p*-fluorophenyl group, large and polar substituents are generally not well tolerated and they typically result in loss of activity for analogues such as **7f**–**h**. While an *o*-substituent on the 4-phenyl group is expected to take an opposite position to the 4-methyl group on the core, it will elicit steric clash with the side chain of Thr128 and makes analogues such as **7c** much less active. Importantly, the methyl group of the 5-ester contacts the outer rim of a pocket formed by Leu37 and Thr109 so that polar and large groups may not be favored at this position (examples **27a**–**f**).

The 4,4-difluoroproline group is partially solvent-exposed, however, the *gem*-fluoro substituents interact with Trp125', Thr128', Arg133' and Pro134' and the carboxylic acid moiety make bidentate HB interactions with Ser141. Those interactions could contribute to the high binding affinity of **34a** to capsid proteins and its increased anti-HBV activity. In contrast, amino ester analogue **34f** and 2*R*-diastereoisomer **34c** cannot make bidentate HB interactions with Ser141 in the binding site and both of them had reduced activities relative to **34a**. Moreover, a water-bridged HB network exists between the 2-thiazole and carboxyl groups of **34a** (Figure 3). This well-defined water molecule, as well as the HB formed between the dihydropyrimidine core and Trp102, are also noted in the recent co-crystal structure of the *N*-terminal assembly domain of the HBV capsid protein in complex with 4-H HAP analogue **3** (PDB 5E0I).[12] Interestingly, besides the molecule of **34a** binding to the dimer-dimer interface, an additional molecule was identified at the A-B spike probably due to the excess of ligand during the crystallization setup (Figure. S3 in Supporting Information).

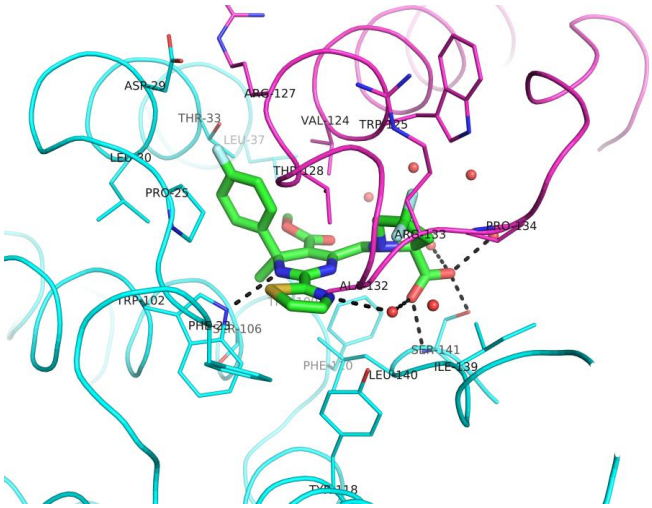

Figure 3. Binding site of **34a** with HBV capsid protein Y132A. The compound binding pocket at B-C interface is shown as an exemplary site. Chain B and Chain C of Y132A-**34a** structure are colored in cyan and magenta respectively. Compound **34a** is highlighted in green stick. Residues within 4 Å radius are shown as lines. Red spheres represent water molecules in the pocket. Black dash lines indicate hydrogen bonds between **34a** and core protein.

Section 8. DMPK and In Vivo Efficacy of 34a. Amino acid analogue **34a** had desirable in vitro potency and physicochemical properties with a polar surface area (PSA) of 85 $Å^2$ and a measured logD of 0.25. Since the "zwitterionic" structural features of **34a** are often associated with permeability issues, we carried out mechanistic and SDPK studies of **34a**. Compound **34a** had a P_{app} (A→B) of 1.9 $\times 10^{-6}$ cm s^{-1} and P_{app} ratio of 3.6 in the Caco-2 assay. The unbound fraction of **34a** was determined to be 1.9% and 8.1% in human and mouse plasma, respectively. The SDPK profile of **34a** was evaluated in CD-1 mice following intravenous (i.v.) and oral (p.o.) administration. **34a** had moderate plasma clearance (*Cl*) (55.3 mL min^{-1} kg^{-1}) with an oral bioavailability (*F*) of 36% in mice (Table 6). In particular, **34a** had a high exposure in the liver with an area under the curve ($AUC_{(0-t)}$) of 107000 μg L^{-1} hr^{-1} and very limited tissue distribution to lung, heart and brain. The liver exposure of **34a** was about 20 times higher than that in plasma by oral administration. In contrast, **1** is not stable in liver homogenate so its liver exposure could not be determined (data not included). The preferential liver distribution of **34a** could be a useful characteristic in treating chronic HBV infections, where the disease organ is the liver.

In addition, **34a** exhibits low CYP inhibition with IC_{50}s > 30 μM against five major CYP enzymes (3A4, 2D6, 2C9, 2C19, 1A2) and was also not a time dependent CYP inhibitor. Moreover, **34a** did not significantly inhibit the hERG ion channel with IC_{20} > 10 μM and was negative in preliminary in vitro safety evaluations such as glutathione (GSH) adduct, Ames, as well as micronucleus test (MNT) assays. In contrast, compound **1** and non-carboxylic acid 4-methyl HAP analogues (*S*)-**18a** and **31m** were tested positive in GSH adduct assays. Our mechanistic studies indicated that **34a** induces capsid assembly (or aggregation) of the *N*-terminal capsid assembly domain (Cp149) in a concentration dependent manner, in agreement with previous reports on the 4-H HAP-based capsid inhibitors (see the Supporting Information).[7, 13]

Table 6. ADME Parameters of 4-Methyl HAP **34a** in CD-1 Mice[a]

Parameters	Dose (mg/kg)	CL (mL min^{-1} kg^{-1})	Vss (L/kg)	$t_{1/2}$ (h)	Plasma_Cmax (μg/L)	Plasma_AUC$_{(0-t)}$ (μg L^{-1} hr^{-1})	Liver_Cmax (μg/L)	Liver_AUC$_{(0-t)}$ (μg L^{-1} hr^{-1})	F (%)
i.v.	5	55.3	0.22	0.18	12400	1500			
p.o.	50			0.8	2470	5420	41200	107000	36

[a] The single-dose pharmacokinetics (SDPK) study of **34a** was carried out in CD-1 mice according to standard procedures. Major parameters, including plasma clearance (*Cl*), volume of distribution at steady state (Vss), $t_{1/2}$ (i.v.), maximal concentration (C_{max}), area under the curve (AUC), and oral bioavailability (*F*) are reported.

Finally, the in vivo efficacy of **34a** was evaluated in BALB/c mice that underwent hydrodynamic injection (HDI) with replication-competent HBV DNA plasmid.[24] Entecavir (ETV, 0.1 mg/kg) was used as the positive control in the HDI experiment. HBV replication was quickly built up in the liver of HDI mice after injection of the HBV plasmid and the levels of HBV DNA were determined by real-time PCR. As shown in Figure 4A, **34a** demonstrated dose-dependent reduction of HBV DNA in the plasma of infected mice when the compound was orally administered twice a day (b.i.d.) at 12.5 mg/kg (mpk), 25 mpk and 50 mpk, respectively. In comparison to the vehicle control group, treatment with 50 mpk of **34a** b.i.d. achieved over 2-log viral load reduction in the plasma of HDI mice on day 5.

The levels of HBV DNA in mouse liver were determined 5 days post hydrodynamic injection of the HBV DNA plasmid (Figure 4B). The liver DNA was isolated and subjected to real-time PCR for quantification of HBV DNA. Consistent with the results in mouse plasma, **34a** dose-dependently reduced HBV DNA levels in the mouse liver, achieving levels comparable to the positive control on day 5 with oral dosing at 50 mpk b.i.d.

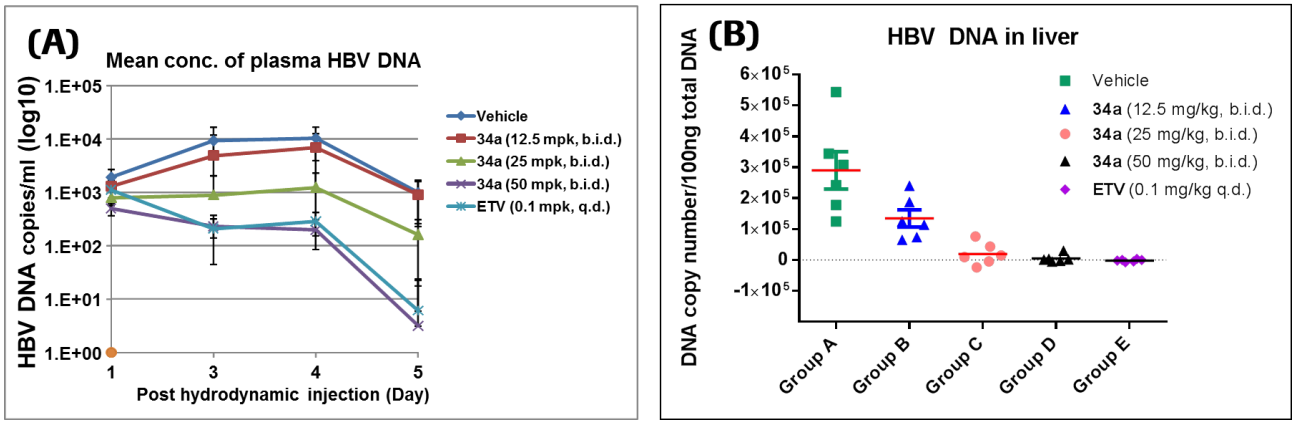

Figure 4. The levels of HBV DNA in the plasma (A) and liver (B) of infected mice. Treatments with the vehicle control, **34a** and ETV are included. The HBV DNA was quantified by real-time PCR. Error bars represent standard error. Statistical analysis was done by Student's t test. * P< 0.001.

CONCLUSIONS

In summary, we have identified a novel class of 4-methyl HAP-based HBV capsid inhibitors by an information-driven strategy. A highly efficient synthetic method was developed for SAR and structure–property relationship (SPR) studies with the aim to improve the in vitro anti-HBV activity and cytotoxicity profile, and to optimize physicochemical properties. Structural optimization resulted in the identification of (2*S*, 4*S*)-4,4-difluoroproline substituted analogue **34a**, which exhibited an EC_{50} value of 84 nM and an over 1900-fold selectivity margin in HepDE19 cells. In particular, this kind of zwitterionic compound had good plasma stability and oral bioavailability with high liver exposure in mice. In in vivo studies, **34a** dose-dependently reduced HBV DNA in both the plasma and liver of HBV-infected HDI mice, achieving over 2-log viral load reduction on day 5 with 50 mpk b.i.d. dosing. Future optimizations of **34a** include core modifications and peripheral substituent changes with the specific aim to reduce efficacious doses.

In the course of SAR exploration, it was noted that minor changes in HAP structure can have profound effects on the capsid assembly or aggregation process and thus inhibition of HBV DNA synthesis. A co-crystal structure of **34a** and Y132A mutant capsid protein was obtained with 1.7Å

resolution, clearly elucidating the binding mode of **34a** and importantly, the role that the (2*S*)-4,4-difluoroproline group plays in protein-ligand interactions. Specifically, the fluorine atoms make important VDW contacts with Trp125', Thr128', Arg133' and Pro134' of the capsid protein and the carboxylic acid moiety forms bidentate HB interactions with Ser141. The SAR, biostructure, SPR, DMPK and in vivo efficacy studies of 4-methyl HAP analogues like **34a** provide valuable information for further structural optimizations of the HAP scaffold in our endeavor to identify and develop highly efficacious and safe HBV capsid inhibitors, the results of which will be published in due course.

EXPERIMENTAL SECTION

Synthetic Chemistry General Comments. All of the intermediates were purified by silica gel chromatography using either a Biotage SP1 system or an ISCO CombiFlash chromatography instrument. All of the final compounds were purified by preparative HPLC (prep-HPLC) on a reversed-phase column using a Waters XBridge OBD Phenyl (30 mm × 100 mm, 5 μm) or OBD RP18 (30 mm × 100 mm, 5 μm) column under acidic conditions (A, 0.1% formic acid in H_2O; B, 0.1% formic acid in acetonitrile) or basic conditions (A, 0.01% ammonia in H_2O; B, acetonitrile). For SFC chiral separation, the intermediates were separated using a chiral column (Daicel Chiralpak IC, 30 mm × 250 mm, 5 μm) on a Mettler Teledo SFC-Multigram system (solvent system of 95% CO_2 and 5% IPA (0.5% TEA in IPA), backpressure of 100 bar, UV detection at 254 nm). Optical rotation was measured using a Rudolph Autopol V automatic polarimeter at a wavelength of 589 nm. LC−MS spectra were obtained using a MicroMass Platform LC (Waters Alliance 2795-ZQ2000). NMR spectra were obtained using a Bruker Avance 400 MHz NMR spectrometer. All of the starting materials were obtained commercially, and amidines **12** were prepared in house according to literature reported methods (see the Supporting Information). All of the final compounds have purities greater than 95% based upon LC−MS and ^{1}H NMR analyses. All of the reported yields are for isolated products and are not optimized.

General Synthetic Procedures for 4-Methyl HAP Analogues 7a−i: A mixture of methyl 3-oxobutanoate (compound **8**, 10 mmol) and a benzaldehyde derivative **9** (10 mmol), piperidine (0.5 mmol) and AcOH (0.5 mmol) in anhydrous EtOH (100 mL) was stirred at rt for 12 h. After removal of the solvent, the residue was purified by flash chromatography to afford the aldol condensation product, which was then dissolved in 50 mL of anhydrous THF and added dropwise to a fresh prepared THF solution of CH_3CuLi (2 eq.) at −78 ℃. The reaction mixture was stirred for 1 h and quenched with saturated NH_4Cl solution. The aqueous solution was extracted with EtOAc and the combined organic phase was concentrated. The residue was purified by flash column chromatography to give β-ketoester **10**.

To a solution of NaH (60%, 15 mmol) and **10** (10 mmol) in anhydrous THF (100 mL) was added a solution of phenylselenyl chloride (15 mmol) in THF (20 mL), and the reaction mixture was stirred at rt for 1 h. A mixture of pentene/ether (v/v =1/1, 60 mL) and 30 mL of saturated $NaHCO_3$ solution were added to the flask. The organic layer was separated and then treated with H_2O_2 (30%, 2 mL) in 30 mL of DCM. The mixture was stirred at rt for 1 h and diluted with DCM before workup. Tetra-substituted olefin **11** was obtained as yellowish oil after purification by flash chromatography.

A mixture of amidine **12** (10 mmol) and $NaHCO_3$ (20 mmol) in 15 mL of NMP was preheated to 120 ℃, and to this stirring mixture was added dropwise a solution of **11** (10 mmol) in NMP (5 mL). The reaction mixture was stirred at 120 ℃ for 2 h before it was cooled to rt and diluted with water. The aqueous phase was extraced with EtOAc and the combined organic phase was washed with brine, dried over anhydrous Na_2SO_4 and concentrated. The residue was purified by flash column chromatography to afford **7a−i** as powder.

*Methyl (4S)-(4-fluorophenyl)-4,6-dimethyl-2-(2-methylthiazol-4-yl)-1H-pyrimidine-5-carboxylate [(S)-**7a**]*. *(S)*-**7a** was obtained by chiral SFC separation. Optical rotation: $[\alpha]_D^{20}$ = 75.6 (1.0 mg/mL, MeOH). MS: calcd (MH^+) 346.1, exp (MH^+) 346.1. HRMS: calcd (MH^+) 346.1020, exp (MH^+) 346.1020. ^1H

NMR (Methanol-d_4) δ 7.93 (d, J = 3.3 Hz, 1H), 7.72 (d, J = 3.3 Hz, 1H), 7.52−7.46 (m, 2H), 7.07−7.00 (m, 2H), 3.45 (s, 3H), 2.28 (s, 3H), 1.90 (s, 3H).

*Methyl 2-(3,5-difluoro-2-pyridyl)-4-(4-fluorophenyl)-4,6-dimethyl-1H-pyrimidine-5-carboxylate (**7b**).* MS: calcd (MH^+) 376.1, exp (MH^+) 376.1. HRMS: calcd (MH^+) 376.1267, exp (MH^+) 376.1269. ^{1}H NMR (Methanol-d_4) δ 8.46 (d, J = 2.5 Hz, 1 H), 7.71 (ddd, J = 9.8, 8.6, 2.3 Hz, 1 H), 7.53 (dd, J = 9.1, 5.3 Hz, 2 H), 7.04 (t, J = 8.8 Hz, 2 H), 3.45 (s, 3 H), 2.24 (s, 3 H), 1.92 (s, 3 H).

*Methyl 4-(2-chloro-4-fluoro-phenyl)-4,6-dimethyl-2-thiazol-2-yl-1H-pyrimidine-5-carboxylate (**7c**).* MS: calcd (MH^+) 380.1, exp (MH^+) 380.1. ^{1}H NMR (Methanol-d_4) δ 7.95 (d, J = 3.2 Hz, 1H), 7.72 (d, J = 3.2 Hz, 1H), 7.70−7.67 (m, 1H), 7.15−7.08 (m, 2H), 3.51 (s, 3H), 2.3 (s, 3H), 1.95 (s, 3H).

*Methyl 4,6-dimethyl-4-phenyl-2-thiazol-2-yl-1H-pyrimidine-5-carboxylate (**7d**).* MS: calcd (MH^+) 328.1, exp (MH^+) 328.1. ^{1}H NMR (Methanol-d_4) δ 7.93 (d, J = 3.3 Hz, 1H), 7.73 (d, J = 3.3 Hz, 1H), 7.49 (dd, J = 8.5, 1.1 Hz, 2H), 7.32 (t, J = 7.7 Hz, 2H), 7.24−7.17 (m, 1H), 3.42 (s, 3H), 2.28 (s, 3H), 1.92 (s, 3H).

*Methyl 4-(4-chlorophenyl)-4,6-dimethyl-2-thiazol-2-yl-1H-pyrimidine-5-carboxylate (**7e**).* MS: calcd (MH^+) 362.1, exp (MH^+) 362.1. ^{1}H NMR (Methanol-d_4) δ 7.93 (d, J = 3.0 Hz, 1H), 7.71 (d, J = 3.0 Hz, 1H), 7.44 (d, J = 8.6 Hz, 2H), 7.31 (d, J = 8.6 Hz, 2H), 3.45 (s, 3H), 2.29 (s, 3 H), 1.88 (s, 3H).

*Methyl 4,6-dimethyl-4-(4-methylsulfonylphenyl)-2-thiazol-2-yl-1H-pyrimidine-5-carboxylate (**7f**).* MS: calc'd (MH^+) 436.1, exp (MH^+) 436.1. ^{1}H NMR (Methanol-d_4) δ 7.94 (d, J = 3.3 Hz, 1H), 7.91 (d, J = 8.3 Hz, 2H), 7.75 (d, J = 8.6 Hz, 2H), 7.71 (d, J = 3.3 Hz, 1H), 3.45 (s, 3H), 3.12 (s, 3H), 2.34 (s, 3H), 1.93 (s, 3H).

*Methyl 4-(4-methoxyphenyl)-4,6-dimethyl-2-thiazol-2-yl-1H-pyrimidine-5-carboxylate (**7g**).* MS: calcd (MH^+) 358.1, exp (MH^+) 358.1. ^{1}H NMR (Methanol-d_4) δ 7.93 (d, J = 3.0 Hz, 1H), 7.72 (m, 1H), 7.39 (m, 2H), 6.88 (d, J = 8.6 Hz, 2H), 3.79 (s, 3H), 3.44 (s, 3H), 2.26 (s, 3H), 1.89 (s., 3H).

*Methyl 4-(4-cyanophenyl)-4,6-dimethyl-2-thiazol-2-yl-1H-pyrimidine-5-carboxylate (**7h**).* MS: calcd (MH^+) 353.1, exp (MH^+) 353.1. HRMS: calcd (MH^+) 353.1067, exp (MH^+) 353.1068. ^{1}H NMR (Methanol-d_4) δ 7.93 (d, J = 3.3 Hz, 1H), 7.73−7.62 (m, 5H), 3.44 (s, 3H), 2.33 (s, 3H), 1.90 (s, 3H).

*Methyl 4-(3,4-difluorophenyl)-4,6-dimethyl-2-thiazol-2-yl-1H-pyrimidine-5-carboxylate (**7i**).* MS: calcd (MH^+) 364.1, exp (MH^+) 364.1. HRMS: calcd (MH^+) 364.0926, exp (MH^+) 364.0925. ^{1}H NMR (Methanol-d_4) δ 7.94 (d, J = 3.0 Hz, 1H), 7.72 (d, J = 3.3 Hz, 1H), 7.36−7.14 (m, 3H), 3.48 (s, 3H), 2.30 (s, 3H), 1.86 (s, 3H).

Synthesis of 4-Ethyl HAP Analogue 7j. To a mixture of 1-(4-fluorophenyl)propan-1-one (compound **13**, 0.1 mol) in 100mL of EtOH was added $NaBH_4$ (0.2 mol) and the mixture was stirred at rt for 2 h. After removal of the solvent, the residue was treated with saturated Na_2CO_3 solution and extracted with EtOAc. The organic phase was washed with brine, dried over anhydrous Na_2SO_4 and concentrated. The crude product was dissolved in 200 mL of DCM and to this solution was added thionyl chloride (0.2 mol) at 0 ℃. After 3 h of stirring at rt, the mixture was concentrated and benzyl chloride **14** was obtained as yellowish oil.

To a mixture of **8** (2.9 mmol) in THF (20 mL) was added NaH (60%, 3.5 mmol) and the reaction mixture was stirred at 0 ℃ for 20 min. Chloride **14** (2.9 mmol) was added into the flask and the resulted mixture was stirred at rt for 12 h before it was quenched with 5 mL of brine. The organic layer was separated and concentrated. The residue was purified by flash chromatography to afford methyl 2-acetyl-3-(4-fluorophenyl)pentanoate (**15**) in 60% yield. MS: exp (MH^+) 253.3.

Methyl 2-acetyl-3-(4-fluorophenyl)pent-2-enoate (**16**) was obtained as a mixture of E/Z isomers from **15** by the two-step phenylselenation and oxidation reactions as described previously. To a mixture of thiazole-2-carboxamidine hydrochloride (0.4 mmol) and AcOK (0.4 mmol) in 5 mL of isopropanol was added a solution of **16** (0.4 mmol) in 2 mL of isopropanol at 120 ℃. The reaction mixture was stirred at 120 ℃ for 3 h before concentrated in vacuum. The residue was purified by prep-HPLC to afford **7j** as yellowish solid in 15% yield.

Methyl 4-ethyl-4-(4-fluorophenyl)-6-methyl-2-thiazol-2-yl-1H-pyrimidine-5-carboxylate ***(7j)***. MS: calcd (MH^+) 360.1, exp (MH^+) 360.1. HRMS: calcd (MH^+) 360.1182, exp (MH^+) 360.1191. ^{1}H NMR (Methanol-d_4) δ 7.97 (d, J = 8.0 Hz, 1H), 7.72 (d, J = 8.0 Hz, 1H), 7.49−7.45 (m, 2H), 7.04−7.00 (m, 2H), 3.51 (s, 3H), 2.65 (m, 1H), 2.30(s, 3H), 2.04 (m, 1H), 1.00 (m, 3H)

General Procedures for the Synthesis of 6-Morpholine Substituted Analogues 18a−k. To a solution of intermediates **7** (3 mmol) and DMAP (1.5 mmol) in 20 mL of DCM was added Boc_2O (4.5 mmol), and the mixture was stirred at rt overnight. The organic phase was washed with water and brine, dried over anhydrous Na_2SO_4 and concentrated. The residue was purified by flash chromatography to afford the *N*-Boc protected intermediate in quantitative yield. The product was dissolved in 30 mL of CCl_4. To this solution was added NBS (3 mmol) and the mixture was brought to 50 ℃. AIBN (30 mg) was added to the flask and the mixture was stirred at 50 ℃ for 2 h. The mixture was filtered through silic gel and washed with EtOAc. The filtrate was concentrated to afford **17** as yellowish powder and it was used for the next reaction directly.

To a solution of **17** (1 mmol) in 20 mL of DCM was added morpholine (0.5 mL) and the mixture was stirred at 50 ℃ for 1 h. After concentration, the residue was dissolved in EtOAc and washed with 1N HCl and brine. The organic phase was concentrated and the residue was dissolved in 20 mL of DCM. To this solution was added TFA (1 mL) and the mixture was stirred at rt for 2 h. After removal of the solvent, the residue was purified by prep-HPLC to afford **18a−k**.

*(S)-4-(4-Fluoro-phenyl)-4-methyl-6-morpholin-4-ylmethyl-2-thiazol-2-yl-1,4-dihydro-pyrimidine-5-carboxylic acid methyl ester [(S)-**18a**]*. (*S*)-**18a** was obtained in together with (*R*)-**18a** by the SFC chiral separation of racemic **18a**. Optical rotation: $[\alpha]_D^{20}$ = 70.5 (1.0 mg/mL, MeOH). MS: calcd (MH^+) 431.1, exp (MH^+) 431.1. HRMS: calcd (MH^+) 431.1548, exp (MH^+) 431.1550. ^{1}H NMR (Methanol-d_4) δ 7.96 (d, J = 3.0 Hz, 1H), 7.74 (d, J = 3.3 Hz, 1H), 7.52−7.43 (m, 2H), 7.03 (t, J = 8.8 Hz, 2H), 3.78 (t, J = 4.4 Hz, 4H), 3.64 (d, J = 17.1 Hz, 1H), 3.60 (d, J = 16.2 Hz, 1H), 3.46 (s, 3H), 2.55−2.60 (m, 4H), 1.90 (s, 3H).

*(R)-4-(4-Fluoro-phenyl)-4-methyl-6-morpholin-4-ylmethyl-2-thiazol-2-yl-1,4-dihydro-pyrimidine-5-carboxylic acid methyl ester [(R)-**18a**]*. $[\alpha]_D^{20}$ = −68.0 (0.95 mg/mL, MeOH). (*R*)-**18a** had identical ^{1}H NMR spectra as (*S*)-**18a**.

*Methyl (4S)-4-(3,4-difluorophenyl)-4-methyl-6-(morpholinomethyl)-2-thiazol-2-yl-1H-pyrimidine-5-carboxylate [(S)-**18b**]*. (*S*)-**18b** and (*R*)-**18b** were obtained by the SFC chiral separation of racemic **18b**. They had identical ^{1}H NMR spectra. MS: calcd (MH^+) 449.1, exp (MH^+) 449.1. HRMS: calcd (MH^+) 449.1453, exp (MH^+) 449.1452. ^{1}H NMR (Methanol-d_4) δ 7.97 (d, *J* = 3.3 Hz, 1H), 7.75 (d, *J* = 3.3 Hz, 1H), 7.33 (ddd, *J* = 12.4, 7.8, 2.3 Hz, 1H), 7.14−7.28 (m, 2H), 3.79 (t, *J* = 4.6 Hz, 4H), 3.59−3.74 (m, 2H), 3.50 (s, 3H), 2.52−2.67 (m, 4H), 1.88 (s, 3H).

*Methyl 4-(3-chloro-4-fluoro-phenyl)-4-methyl-6-(morpholinomethyl)-2-thiazol-2-yl-1H-pyrimidine-5-carboxylate (**18c**).* MS: calcd (MH^+) 465.1, exp (MH^+) 465.1. HRMS: calcd (MH^+) 465.1158, exp (MH^+) 465.1155. ^{1}H NMR (Methanol-d_4) δ 7.97 (d, *J* = 3.3 Hz, 1H), 7.76 (d, *J* = 3.0 Hz, 1H), 7.52 (dd, *J* = 7.2, 2.4 Hz, 1H), 7.41 (ddd, *J* = 8.7, 4.6, 2.4 Hz, 1H), 7.18 (t, *J* = 8.8 Hz, 1H), 3.79 (t, *J* = 4.5 Hz, 4H), 3.75−3.60 (m, 2H), 3.50 (s, 3H), 2.63−2.54 (m, 4H), 1.88 (s, 3H).

*Methyl 4-(4-fluorophenyl)-4-methyl-2-(1-methylimidazol-2-yl)-6-(morpholinomethyl)-1H-pyrimidine-5-carboxylate (**18d**).* MS: calcd (MH^+) 428.2, exp (MH^+) 428.2. HRMS: calcd (MH^+) 428.2098, exp (MH^+) 428.2099. ^{1}H NMR (Methanol-d_4) δ 7.49 (m, 2H), 7.19 (m, 1H), 7.04 (m, 3H), 3.91 (s, 3H), 3.76 (m, 4H), 3.60 (m, 2H), 3.48 (s, 3H), 2.55 (m, 4H), 1.89 (s, 3H).

*Methyl 4-(4-fluorophenyl)-4-methyl-2-(5-methyloxazol-2-yl)-6-(morpholinomethyl)-1H-pyrimidine-5-carboxylate (**18e**).* MS: calcd (MH^+) 429.2, exp (MH^+) 429.2. ^{1}H NMR (Methanol-d_4) δ 7.47 (m, 2H), 7.04 (m, 3H), 3.79 (m, 4H), 3.65 (m, 2H), 3.46 (s, 3H), 2.57 (m, 4H), 2.41 (s, 3H), 1.91 (s, 3H).

*Methyl 4-(4-fluorophenyl)-2-(5-fluoro-2-pyridyl)-4-methyl-6-(morpholinomethyl)-1H-pyrimidine-5-carboxylate (**18f**).* MS: calcd (MH^+) 443.2, exp (MH^+) 443.2. HRMS: calcd (MH^+) 443.1894, exp (MH^+) 443.1889. ^{1}H NMR (Methanol-d_4) δ 8.58 (m, 1H), 8.22 (m, 1H), 7.70 (m, 1H), 7.47 (m, 2H), 7.03 (m, 2H), 3.79 (m, 4H), 3.65 (m, 2H), 3.46 (s, 3H), 2.59 (m, 4H), 1.90 (s, 3H).

*Methyl 4-(4-fluorophenyl)-4-methyl-2-(3-methyl-2-pyridyl)-6-(morpholinomethyl)-1H-pyrimidine-5-carboxylate (**18g**)*. MS: calcd (MH^+) 439.2, calcd (MH^+) 439.2. ^{1}H NMR (Methanol-d_4) δ 8.50 (m, 1H), 7.76 (m, 1H), 7.57 (m, 2H), 7.45 (m, 1H), 7.08 (m, 2H), 3.78 (m, 4H), 3.52 (m, 5H), 2.52 (m, 7H), 1.98 (s, 3H).

*Methyl 4-(4-fluorophenyl)-2-(5-methoxy-2-pyridyl)-4-methyl-6-(morpholinomethyl)-1H-pyrimidine-5-carboxylate (**18h**)*. MS: calcd (MH^+) 455.2, exp (MH^+) 455.2. ^{1}H NMR (Methanol-d_4) δ 8.36 (m, 1H), 8.11 (m, 1H), 7.47 (m, 3H), 7.03 (m, 2H), 3.95 (s, 3H), 3.80 (m, 4H), 3.64 (m, 2H), 3.45 (s, 3H), 2.58 (m, 4H), 1.89 (s, 3H).

*Methyl 4-(4-fluorophenyl)-4-methyl-6-(morpholinomethyl)-2-pyrimidin-2-yl-1H-pyrimidine-5-carboxylate (**18i**)*. MS: calcd (MH^+) 426.2, calcd (MH^+) 426.2. HRMS: calcd (MH^+) 426.1936, exp (MH^+) 426.1934. ^{1}H NMR (Methanol-d_4) δ 8.94 (m, 2H), 7.60 (m, 1H), 7.49 (m, 2H), 7.02 (m, 2H), 3.79 (m, 4H), 3.66 (m, 2H), 3.48 (s, 3H), 2.61 (m, 4H), 1.94 (s, 3H).

*Methyl 4-(4-fluorophenyl)-4-methyl-2-(6-methylpyridazin-3-yl)-6-(morpholinomethyl)-1H-pyrimidine-5-carboxylate (**18j**)*. MS: calcd (MH^+) 440.4, exp (MH^+) 440.2. ^{1}H NMR (Methanol-d_4) δ 8.30−8.22 (m, 1H), 7.73−7.68 (m, 1H), 7.53−7.44 (m, 2H), 7.04 (s, 2H), 3.81 (br t, J = 4.6 Hz, 4H), 3.78−3.61 (m, 2H), 3.47 (s, 3H), 2.77 (s, 3H), 2.68−2.54 (m, 4H), 1.93 (s, 3H).

*Methyl 2-cyclopropyl-4-(4-fluorophenyl)-4-methyl-6-(morpholinomethyl)-1H-pyrimidine-5-carboxylate (**18k**)*. MS: calcd (MH^+) 388.2, exp (MH^+) 388.2. HRMS: calcd (MH^+) 388.2036, exp (MH^+) 388.2044. ^{1}H NMR (Methanol-d_4) δ 7.42 (m, 2H), 7.02 (t, J = 8.7 Hz, 2H), 3.72 (m, 4H), 3.42 (s, 3H), 2.55−2.47 (m, 4H), 1.74 (s, 3H), 1.62 (m, 1H), 0.95−0.83 (m, 4H).

Synthesis of Intermediates 21−26. *tert*-Butyl ester **20** was prepared in analogy to **7** by using *tert*-butyl 3-oxobutanoate (**19**) as the starting material. A mixture of **20** (1 mmol) and TFA (1 mL) in 5 mL of DCM was stirred at rt for 3 h. After removal of the solvent, acid **21** was obtained and it was used in the next reaction directly.

*4-(4-Fluorophenyl)-4,6-dimethyl-2-thiazol-2-yl-1H-pyrimidine-5-carboxylic acid (**21**).* MS: calcd (MH^+) 332.1, exp (MH^+) 332.1. ^{1}H NMR (Methanol-d_4) δ 8.24 (m, 2H), 7.69−7.66 (m, 2H), 7.18 (t, J = 8.0 Hz, 2H), 2.43 (s, 3H), 2.21 (s, 3H).

To a solution of **21** (0.45 mmol), HATU (0.9 mmol), and NEt_3 (0.9 mmol) in 15 mL of DCM was added an NH_3 solution (0.5 M in 1,4-dioxane, 1.8 mmol), and the mixture was stirred at rt overnight. The mixture was washed with aqueous $NaHCO_3$ and brine. The organic layer was separated, dried over anhydrous Na_2SO_4 and concentrated. The residue was purified by flash chromatography to afford **22** in 40% yield.

*4-(4-Fluorophenyl)-4,6-dimethyl-2-thiazol-2-yl-1H-pyrimidine-5-carboxamide (**22**).* MS: calcd (MH^+) 331.1, exp (MH^+) 331.1. ^{1}H NMR (Methanol-d_4) δ 7.94 (m, 1H), 7.73−7.57 (m, 3H), 7.03 (m, 2H), 2.10 (s, 3H), 1.84 (s, 3H).

To a solution of **22** (3 mmol) in 10 mL of THF was added TFAA (3 mL), and the mixture was stirred at rt for 3 h. After removal of THF and excess TFAA, the residue was dissolved in MeOH (20 mL). To this solution was added K_2CO_3 (14.5 mmol), and the mixture was stirred at rt for 3 h. The reaction mixture was filtered and washed with EtOAc. The filtrate was concentrated and the residue was purified by flash chromatography to afford **23** as yellowish solid in 87% yield.

*4-(4-Fluorophenyl)-4,6-dimethyl-2-thiazol-2-yl-1H-pyrimidine-5-carbonitrile (**23**).* MS: calcd (MH^+) 313.1, exp (MH^+) 313.1. ^{1}H NMR (Methanol-d_4) δ 7.96 (m, 1H), 7.76 (m, 1H), 7.51 (m, 2H), 7.11 (m, 2H), 2.23 (s, 3H), 1.83 (s, 3H).

To a solution of **21** (0.5 mmol) in 5 mL of THF was added CDI (0. 6 mmol) and the mixture was stirred at rt for 1 h. After removal of the solvent, the residue was treated with water and the aqueous solution was extracted with EtOAc. The organic layer was dried over anhydrous Na_2SO_4 and concentrated. A mixture of the imidazole amide intermediate (0.4 mmol), methylamine HCl salt (0.8 mmol) and NEt_3 (0.2 mL) in 5 mL of CH_3CN was stirred at 90 ℃ for 30 min in a microwave reactor.

After removal of the solvent, the residue was purified by flash chromatography to afford **24** in 80% yield.

4-(4-Fluorophenyl)-N,4,6-trimethyl-2-thiazol-2-yl-1H-pyrimidine-5-carboxamide ***(24).*** MS: calcd (MH^+) 345.1, exp (MH^+) 345.1. ^{1}H NMR (Methanol-d_4) δ 7.94 (m, 1H), 7.72−7.54 (m, 3H), 7.02 (m, 2H), 2.59 (s, 3H), 2.00 (s, 3H), 1.80 (s, 3H).

A mixture of the oxazole amide intermediate (0.5 mmol), 2,2-dimethoxy-ethylamine (1.0 mmol) in 5 mL of CH_3CN was stirred at 120 ℃ for 30 min in a microwave reactor. After removal of the solvent, the residue was partitioned between water and DCM and the aqueous phase was extracted with DCM. The organic layer was dried over anhydrous Na_2SO_4 and concentrated to give **25** as oil in 90% yield. A mixture of **25** (0.45 mmol) and PPA (5 mL) was stirred at 120 ℃ for 2 h. After cooling down, the mixture was poured to ice water, treated with concentrated NH_3 solution and the aqueous phase was extracted with EtOAc. The organic layer was dried over anhydrous Na_2SO_4 and concentrated. The residue was purified by flash chromatography to give **26** as powder in 30% yield.

2-[4-(4-Fluorophenyl)-4,6-dimethyl-2-thiazol-2-yl-1H-pyrimidin-5-yl]oxazole ***(26)***. MS: calcd (MH^+) 355.1, exp (MH^+) 355.1. ^{1}H NMR (Methanol-d_4) δ 7.95−7.94 (m, 1H), 7.79−7.70 (m, 2H), 7.58−7.46 (m, 2H), 7.11−6.95 (m, 3H), 2.13 (s, 3H), 1.86 (s, 3H).

General Procedures for the Synthesis of Analogues 27a−f. The morpholine-substituted analogues **27a−e** were synthesized by two-step bromination and morpholine substitution of 4-methyl HAP intermediates **21−26**. To a solution of this intermediate (**21−26**, 5 mmol) in 30 mL of CCl_4 were added NBS (5.5 mmol) and AIBN (50 mg) and the mixture was stirred at 50 ℃ for 2 h. After that, morpholine (1.0 mL) was added to the flask and the reaction mixture was stirred at 50 ℃ for 1 h. After removal of the solvent, the residue was partitioned between EtOAc and water. The organic phase was washed with brine and concentrated. The residue was purified by prep-HPLC to afford **27a−e**.

4-(4-Fluorophenyl)-4-methyl-6-(morpholinomethyl)-2-thiazol-2-yl-1H-pyrimidine-5-carboxylic acid ***(27a)***. MS: calcd (MH^+) 417.2, exp (MH^+) 417.2. HRMS: calcd (MH^+) 417.1396, exp (MH^+) 417.1402.

^{1}H NMR (Methanol-d_4) δ 8.00−7.99 (d, J = 4.0 Hz, 1H), 7.89−7.88 (d, J = 4.0 Hz, 1H), 7.65−7.61 (m, 2H), 7.13−7.09 (t, J = 8.0 Hz, 2H), 4.46 (m, 2H), 4.04−4.02 (m, 4H), 3.52 (m, 4H), 2.12 (s, 3H).

*4-(4-Fluorophenyl)-4-methyl-6-(morpholinomethyl)-2-thiazol-2-yl-1H-pyrimidine-5-carboxamide (**27b**)*. MS: calcd (MH^+) 416.2, exp (MH^+) 416.2. HRMS: calcd (MH^+) 416.1556, exp (MH^+) 416.1558. ^{1}H NMR (Methanol-d_4) δ 7.99−7.98 (d, J = 4.0 Hz, 1H), 7.83−7.82 (d, J = 4.0 Hz, 1H), 7.66−7.62 (m, 2H), 7.12−7.08 (m, 2H), 3.89 (m, 6H), 3.16−3.11 (m, 4H), 1.97 (s, 3H).

*4-(4-Fluorophenyl)-4-methyl-6-(morpholinomethyl)-2-thiazol-2-yl-1H-pyrimidine-5-carbonitrile (**27c**).* MS: calcd (MH^+) 398.2, exp (MH^+) 398.2. HRMS: calcd (MH^+) 398.1445, exp (MH^+) 398.1448. ^{1}H NMR (Methanol-d_4) δ 7.99−7.98 (m, 1H), 7.80 (m, 1H), 7.53−7.49 (m, 2H), 7.14−7.09 (m, 2H), 3.76(m, 4H), 3.50 (m, 2H), 2.56 (m, 4H), 1.85 (s, 3H).

*4-(4-Fluorophenyl)-N,4-dimethyl-6-(morpholinomethyl)-2-thiazol-2-yl-1H-pyrimidine-5-carboxamide (**27d**)*. MS: calcd (MH^+) 430.2, exp (MH^+) 430.2. HRMS: calcd (MH^+) 430.1712, exp (MH^+) 430.1711. ^{1}H NMR (Methanol-d_4) δ 7.98−7.97 (d, J = 4.0Hz, 1H), 7.80−7.79 (d, J = 4.0Hz, 1H), 7.60−7.57 (m, 2H), 7.09−7.04 (m, 2H), 3.82 (m, 4H), 3.52−3.48 (m, 2H), 2.93−2.80 (m, 4H), 2.63 (s, 3H), 1.88 (s, 3H).

*4-[[4-(4-Fluorophenyl)-4-methyl-5-oxazol-2-yl-2-thiazol-2-yl-1H-pyrimidin-6-yl]methyl]morpholine (**27e**)*. MS: calcd (MH^+) 440.1, exp (MH^+) 440.1. HRMS: calcd (MH^+) 440.1556, exp (MH^+) 440.1559. ^{1}H NMR (Methanol-d_4) δ 7.98−7.97 (m, 1H), 7.78−7.74 (m, 2H), 7.49 (m, 2H), 7.10 (s, 1H), 6.99 (m, 2H), 3.74 (m, 4H), 3.44 (m, 2H), 2.51 (m, 4H), 1.88 (s, 3H).

Analogue **27f** was synthesized in analogy to **18a** by using isopropyl 3-oxobutanoate as the starting material.

*Isopropyl 4-(4-fluorophenyl)-4-methyl-6-(morpholinomethyl)-2-thiazol-2-yl-1H-pyrimidine-5-carboxylate (**27f**)*. MS: calcd (MH^+) 459.2, exp (MH^+) 459.2. ^{1}H NMR (Methanol-d_4) δ 7.95 (d, J = 3.0 Hz, 1H), 7.73 (d, J = 3.3 Hz, 1H), 7.47 (dd, J = 8.2, 5.4 Hz, 2H), 7.04 (t, J = 8.8 Hz, 2H), 4.86 (m, 2H),

4.78 (dt, J = 12.4, 6.3 Hz, 1H), 3.79 (t, J = 4.6 Hz, 4H), 2.59 (m, 4H), 1.90 (s, 3H), 1.10 (d, J = 6.3 Hz, 3H), 0.82 (d, J = 6.3 Hz, 3H).

General Procedures for the Synthesis of *N*-linked Analogues 31a−t. To a mixture of methyl 3-oxobutanoate (compound **8**, 5.0 g, 43.1 mmol), 1-ethynyl-4-fluoro-benzene (compound **28**, 5.0 g, 41.7mmol) in 20 mL of o-xylene was added $In(OTf)_3$ (400 mg, 0.71 mmol) and the mixture was stirred at 120 ℃ for 1−2 h. After removal of the solvent, the residue was purified by flash chromatography (EtOAc/petroleum ether: 1/10) to afford olefin **29** as light yellowish oil in 40% yield. As described previously, **29** was treated with thiazole-2-carboxamidine and $NaHCO_3$ in NMP at 120 ℃ to give **7a** in 60% yield. The *N*-Boc protected bromide intermediate **30** was prepared in analogy to **17** by using **7a** as the starting material.

To a mixture of **30** (2 mmol) and K_2CO_3 [10 mmol, or *t*-BuOK for less reactive (sulfon)amides] in 10 mL of DMF was added amine **32** (2.00 mmol), and the mixture was stirred at 40 ℃ for 3 h before partitioned between water and EtOAc. The organic phase was washed with brine, dried over anhydrous Na_2SO_4 and concentrated. The crude product was treated with TFA in DCM at rt to remove the *N*-Boc protecting group and analogues **31a−r** were purified by prep-HPLC. For the synthesis of analogues **31s−t**, the crude product was treated with LiOH in MeOH at rt for 2 h before treatment with TFA.

*Methyl 4-(4-fluorophenyl)-4-methyl-6-(1-piperidylmethyl)-2-thiazol-2-yl-1H-pyrimidine-5-carboxylate (**31a**)*. MS: calcd (MH^+) 429.2, exp (MH^+) 429.2. HRMS: calcd (MH^+) 429.1760, exp (MH^+) 429.1766. ^{1}H NMR (Methanol-d_4) δ 7.84 (d, J = 3.0 Hz, 1H), 7.71 (m, 1H), 7.35 (m, 2H), 6.93 (m, 2H), 3.55−3.36 (m, 2H), 3.34 (s, 3H), 2.41 (m, 2H), 1.93−1.36 (m, 9H), 1.20 (m, 2H).

*Methyl 4-(4-fluorophenyl)-4-methyl-6-(piperazin-1-ylmethyl)-2-thiazol-2-yl-1H-pyrimidine-5-carboxylate (**31b**)*. MS: calcd (MH^+) 430.2, exp (MH^+) 430.2. HRMS: calcd (MH^+) 430.1713, exp (MH^+) 430.1723. ^{1}H NMR (Methanol-d_4) δ 7.95 (d, J = 3.0 Hz, 1H), 7.77 (d, J = 2.8 Hz, 1H), 7.47 (m, 2H), 7.04 (t, J = 8.8 Hz, 2H), 3.54 (m, 2H), 3.46 (s, 3H), 3.12 (t, J = 5.0 Hz, 4H), 2.69 (m, 4H), 1.90 (s, 3H).

*Methyl 6-[(3,3-dimethylmorpholin-4-yl)methyl]-4-(4-fluorophenyl)-4-methyl-2-thiazol-2-yl-1H-pyrimidine-5-carboxylate (**31c**)*. MS: calcd (MH^+) 459.2, exp (MH^+) 459.2. HRMS: calcd (MH^+) 459.1866, exp (MH^+) 459.1868. ^{1}H NMR (Methanol-d_4) δ 7.98 (d, J = 3.3 Hz, 1H), 7.75 (d, J = 3.0 Hz, 1H), 7.45 (dd, J = 5.6, 8.8 Hz, 2H), 7.03 (t, J = 9.0 Hz, 2H), 3.90−3.66 (m, 4H), 3.50 (m, 2H), 3.46 (s, 3H), 2.64 (m, 2H), 1.90 (s, 3H), 1.14 (s, 6H).

*Methyl 4-(4-fluorophenyl)-4-methyl-6-(2-oxa-5-azabicyclo[2.2.1]heptan-5-ylmethyl)-2-thiazol-2-yl-1H-pyrimidine-5-carboxylate (**31d**)*. MS: calcd (MH^+) 443.1, exp (MH^+) 443.1. HRMS: calcd (MH^+) 443.1553, exp (MH^+) 443.1555. ^{1}H NMR (Methanol-d_4) δ 7.94 (d, J = 3.0 Hz, 1H), 7.74 (d, J = 3.0 Hz, 1H), 7.47 (t, J = 5.8 Hz, 2H), 7.08−7.00 (m, 2H), 4.51 (m, 1H), 4.10−3.71 (m, 4H), 3.58 (m, 1H), 3.46 (m, 3H), 3.00−2.73 (m, 2H), 2.00 (d, J = 9.9 Hz, 1H), 1.91 (s, 1.5H), 1.90 (s, 1.5H), 1.82 (d, J = 9.9 Hz, 1H).

*Methyl 4-(4-fluorophenyl)-4-methyl-6-[(3-oxomorpholin-4-yl)methyl]-2-thiazol-2-yl-1H-pyrimidine-5-carboxylate (**31e**)*. MS: calcd (MH^+) 445.1, exp (MH^+) 445.1. ^{1}H NMR (DMSO-d_6) δ 9.30 (m, 1H), 8.0−7.92 (m, 2H), 7.52−7.42 (m, 2H), 7.17−7.10 (m, 2H), 4.53−4.36 (m, 2H), 4.15−4.10 (m, 2H), 3.90−3.85 (m, 2H), 3.48−3.43 (m, 5H), 1.94 (s, 3H).

*Methyl 4-(4-fluorophenyl)-4-methyl-6-[(3-oxopiperazin-1-yl)methyl]-2-thiazol-2-yl-1H-pyrimidine-5-carboxylate (**31f**)*. MS: calcd (MH^+) 444.1, exp (MH^+) 444.1. HRMS: calcd (MH^+) 444.1505, exp (MH^+) 444.1512. ^{1}H NMR (Methanol-d_4) δ 7.94 (d, J = 3.0 Hz, 1H), 7.75 (d, J = 2.8 Hz, 1H), 7.48 (dd, J = 8.3, 5.6 Hz, 2H), 7.04 (t, J = 8.7 Hz, 2H), 3.85−3.65 (m, 2H), 3.47 (s, 3H), 3.42 (t, J = 5.2 Hz, 2H), 3.28 (m, 2H), 2.80 (d, J = 2.3 Hz, 2H), 1.91 (s, 3H).

*Methyl 4-(4-fluorophenyl)-6-[(4-hydroxy-1-piperidyl)methyl]-4-methyl-2-thiazol-2-yl-1H-pyrimidine-5-carboxylate (**31g**)*. MS: calcd (MH^+) 445.1, exp (MH^+) 445. HRMS: calcd (MH^+) 445.1709, exp (MH^+) 445.1716. ^{1}H NMR (Methanol-d_4) δ 7.95 (d, J = 3.3 Hz, 1H), 7.74 (d, J = 3.3 Hz, 1H), 7.46 (dd, J = 5.3, 8.6 Hz, 2H), 7.03 (t, J = 8.8 Hz, 2H), 3.79−3.54 (m, 3H), 3.45 (s, 3H), 2.84 (d, J = 11.9 Hz, 2H), 2.35 (q, J = 11.5 Hz, 2H), 2.03−1.87 (m, 5H), 1.76−1.60 (m, 2H).

*Methyl 6-[(1,1-dioxo-1,4-thiazinan-4-yl)methyl]-4-(4-fluorophenyl)-4-methyl-2-thiazol-2-yl-1H-pyrimidine-5-carboxylate (**31h**).* MS: calcd (MH^+) 479.1, exp (MH^+) 479. HRMS: calcd (MH^+) 479.1222, exp (MH^+) 479.1228. ^{1}H NMR (Methanol-d_4) δ 7.98 (d, *J* = 3.3 Hz, 1H), 7.77 (d, *J* = 3.0 Hz, 1H), 7.49 (m, 2H), 7.04 (t, *J* = 8.6 Hz, 2H), 3.95−3.71 (m, 2H), 3.48 (s, 3H), 3.22 (m, 4H), 3.13 (d, *J* = 5.8 Hz, 4H), 1.90 (s, 3H).

*Methyl 6-[(4,4-difluoro-1-piperidyl)methyl]-4-(4-fluorophenyl)-4-methyl-2-thiazol-2-yl-1H-pyrimidine-5-carboxylate (**31i**).* MS: calcd (MH^+) 465.1, exp (MH^+) 465.1. HRMS: calcd (MH^+) 465.1567, exp (MH^+) 465.1568. ^{1}H NMR (Methanol-d_4) δ 7.96 (d, *J* = 3.3 Hz, 1H), 7.75 (d, *J* = 3.0 Hz, 1H), 7.47 (dd, *J* = 8.8, 5.56 Hz, 2H), 7.03 (t, *J* = 8.7 Hz, 2H), 3.80−3.62 (m, 2H), 3.46 (s, 3H), 2.70 (d, *J* = 5.0 Hz, 4H), 2.16−2.03 (m, 4H), 1.90 (s, 3H).

*Methyl 6-[(3,3-difluoro-1-piperidyl)methyl]-4-(4-fluorophenyl)-4-methyl-2-thiazol-2-yl-1H-pyrimidine-5-carboxylate (**31j**).* MS: calcd (MH^+) 465.1, exp (MH^+) 465.1. HRMS: calcd (MH^+) 465.1567, exp (MH^+) 465.1577. ^{1}H NMR (Methanol-d_4) δ 8.03 (d, *J* = 3.3 Hz, 1H), 7.95 (d, *J* = 3.3 Hz, 1H), 7.68−7.59 (m, 2H), 7.17−7.09 (m, 2H), 4.52−4.40 (m, 2H), 3.85−3.69 (m, 2H), 3.50 (s, 3H), 3.45 (t, *J* = 5.3 Hz, 2H), 2.30−2.14 (m, 4H), 2.11 (s, 3H).

*Methyl 4-(4-fluorophenyl)-6-[(3-hydroxypyrrolidin-1-yl)methyl]-4-methyl-2-thiazol-2-yl-1H-pyrimidine-5-carboxylate (**31k**).* MS: calcd (MH^+) 431.1, exp (MH^+) 431.1. HRMS: calcd (MH^+) 431.1553, exp (MH^+) 431.1556. ^{1}H NMR (Methanol-d_4) δ 7.94 (d, *J* = 3.3 Hz, 1H), 7.75 (d, *J* = 2.8 Hz, 1H), 7.48 (m, 2H), 7.04 (t, *J* = 8.7 Hz, 2H), 4.45−4.36 (m, 1H), 3.87−3.69 (m, 2H), 3.46 (d, *J* = 1.5 Hz, 3H), 2.91 (m, 2H), 2.64 (m, 2H), 2.22 (qd, *J* = 13.9, 7.1 Hz, 1H), 1.90 (s, 3H), 1.81 (m, 1H).

*Methyl 6-[(3,3-difluoropyrrolidin-1-yl)methyl]-4-(4-fluorophenyl)-4-methyl-2-thiazol-2-yl-1H-pyrimidine-5-carboxylate (**31m**).* MS: calcd (MH^+) 451.1, exp (MH^+) 451.1. HRMS: calcd (MH^+) 451.1415, exp (MH^+) 451.1416. ^{1}H NMR (Methanol-d_4) δ 7.94 (d, *J* = 3.0 Hz, 1H), 7.74 (d, *J* = 3.0 Hz, 1H), 7.51−7.44 (m, 2H), 7.04 (t, *J* = 8.8 Hz, 2H), 3.87−3.70 (m, 2H), 3.46 (s, 3H), 3.15−3.00 (m, 2H), 2.92 (dt, *J* = 4.5, 6.8 Hz, 2H), 2.37 (tt, *J* = 7.2, 14.7 Hz, 2H), 1.90 (s, 3H).

*Methyl 4-(4-fluorophenyl)-4-methyl-2-thiazol-2-yl-6-{[3-(trifluoromethyl)pyrrolidin-1-yl]methyl}-1H-pyrimidine-5-carboxylate (**31n**).* MS: calcd (MH^+) 483.1, exp (MH^+) 483.1. HRMS: calcd (MH^+) 483.1478, exp (MH^+) 483.1482. ^{1}H NMR (DMSO-d_6) δ 8.09 (d, *J* = 3.0 Hz, 1H), 8.03 (d, *J* = 3.0 Hz, 1H), 7.51 (m, 2H), 7.16 (t, *J* = 8.8 Hz, 2H), 4.41−4.51 (m, 2H), 3.85−3.77 (m, 2H), 3.68−3.59 (m, 3H), 3.43 (m, 3H), 2.30−2.38 (m, 1H), 2.09 (m, 1H), 1.97 (m, 3H).

*Methyl 6-[(1,1-dioxo-1,2-thiazolidin-2-yl)methyl]-4-(4-fluorophenyl)-4-methyl-2-thiazol-2-yl-1H-pyrimidine-5-carboxylate (**31p**).* MS: calcd (MH^+) 465.1, exp (MH^+) 465.1. HRMS: calcd (MH^+) 465.1061, exp (MH^+) 465.1056. ^{1}H NMR (Methanol-d_4) δ 7.93 (m, 1H), 7.83−7.70 (m, 1H), 7.67−7.41 (m, 2H), 7.06 (d, *J* = 7.6 Hz, 2H), 4.41−4.22 (m, 1H), 4.12 (m, 1H), 3.64−3.37 (m, 6H), 3.21 (m, 1H), 2.43 (d, *J* = 6.3 Hz, 2H), 2.02−1.84 (m, 3H).

*Methyl 4-(4-fluorophenyl)-6-(imidazol-1-ylmethyl)-4-methyl-2-thiazol-2-yl-1H-pyrimidine-5-carboxylate (**31q**).* MS: calcd (MH^+) 412.1, exp (MH^+) 412.1. ^{1}H NMR (Methanol-d_4) δ 9.08 (t, *J* = 1.4 Hz, 1H), 7.93 (d, *J* = 3.3 Hz, 1H), 7.79 (d, *J* = 3.0 Hz, 1H), 7.75 (t, *J* = 1.8 Hz, 1H), 7.63−7.55 (m, 3H), 7.11 (t, *J* = 8.8 Hz, 2H), 5.42 (m, 2H), 3.53 (s, 3H), 2.05 (s, 3H).

*Methyl 4-(4-fluorophenyl)-6-[(3-methoxyazetidin-1-yl)methyl]-4-methyl-2-thiazol-2-yl-1H-pyrimidine-5-carboxylate (**31r**).* MS: calcd (MH^+) 431.1, exp (MH^+) 431.1. HRMS: calcd (MH^+) 431.1553, exp (MH^+) 431.1558. ^{1}H NMR (Methanol-d_4) δ 7.98 (d, *J* = 3.3 Hz, 1H), 7.88 (d, *J* = 3.3 Hz, 1H), 7.60 (dd, *J* = 8.8, 5.3 Hz, 2H), 7.11 (t, *J* = 8.7 Hz, 2H), 4.57 (m, 4H), 4.39 (m, 1H), 4.33−4.13 (m, 2H), 3.49 (s, 3H), 3.40 (s, 3H), 2.07 (s, 3H).

*2-{[4-(4-Fluorophenyl)-5-methoxycarbonyl-4-methyl-2-thiazol-2-yl-1H-pyrimidin-6-yl]methyl-methylamino}acetic acid (**31s**).* MS: calcd (MH^+) 433.1, exp (MH^+) 433.1. HRMS: calcd (MH^+) 433.1340, exp (MH^+) 433.1341. ^{1}H NMR (Methanol-d_4) δ 7.96 (d, *J* = 3.0 Hz, 1H), 7.86 (d, *J* = 3.0 Hz, 1H), 7.64−7.58 (m, 2H), 7.12 (t, *J* = 8.8 Hz, 2H), 4.51−4.37 (m, 2H), 3.84 (m, 2H), 3.50 (s, 3H), 3.07 (s, 3H), 2.08 (s, 3H).

*1-{[4-(4-Fluorophenyl)-5-methoxycarbonyl-4-methyl-2-thiazol-2-yl-1H-pyrimidin-6-yl]methyl-methylamino}cyclopropanecarboxylic acid (**31t**)*. MS: calcd (MH^+) 459.1, exp (MH^+) 459.1. HRMS: calcd (MH^+) 459.1502, exp (MH^+) 459.1508. ^{1}H NMR (Methanol-d_4) δ 8.13 (d, J = 3.0 Hz, 1H), 8.07 (d, J = 3.0 Hz, 1H), 7.65−7.57 (m, 2H), 7.15 (t, J = 8.8 Hz, 2H), 4.30 (m, 2H), 3.51 (s, 3H), 2.79 (m, 3H), 2.10 (s, 3H), 1.55−1.48 (m, 2H), 1.41−1.35 (m, 2H).

General Procedures for the Synthesis of *O*-linked Analogues 31u−w. To a stirring mixture of NaH (60%, 0.6 mmol) and alcohol **33** (0.5 mmol) in 20 mL of THF was added **30** and the reaction mixture was stirred at rt overnight. The mixture was partitioned between water and EtOAc. The organic phase was dried over anhydrous Na_2SO_4, concentrated and used in the next step without further purification. The crude product was treated with TFA at rt to remove the *N*-Boc protecting group and the residue was purified by prep-HPLC to afford analogues **31u−v**. For analogue **31w**, the crude product was treated with LiOH in MeOH at rt overnight before treatment with TFA.

*Methyl 4-(4-fluorophenyl)-4-methyl-6-(tetrahydrofuran-3-yloxymethyl)-2-thiazol-2-yl-1H-pyrimidine-5-carboxylate (**31u**)*. MS: calcd (MH^+) 432.1, exp (MH^+) 432.1. HRMS: calcd (MH^+) 432.1393, exp (MH^+) 432.1396. ^{1}H NMR (Methanol-d_4) δ 7.94 (d, J = 3.0 Hz, 1H), 7.74 (d, J = 3.3 Hz, 1H), 7.47 (dd, J = 8.5, 5.4 Hz, 2H), 7.04 (t, J = 8.7 Hz, 2H), 4.76−4.66 (m, 2H), 4.38 (m, 1H), 3.98 (dd, J = 15.3, 8.2 Hz, 2H), 3.91−3.80 (m, 2H), 3.45 (d, J = 1.8 Hz, 3H), 2.18−2.10 (m, 2H), 1.93 (s, 3H).

*Methyl 4-(4-fluorophenyl)-4-methyl-2-thiazol-2-yl-6-(2,2,2-trifluoroethoxymethyl)-1H-pyrimidine-5-carboxylate (**31v**)*. MS: calcd (MH^+) 444.1, exp (MH^+) 444.1. HRMS: calcd (MH^+) 444.1005, exp (MH^+) 444.1006. ^{1}H NMR (Methanol-d_4) δ 7.94 (d, J = 3.0 Hz, 1H), 7.74 (d, J = 3.0 Hz, 1H), 7.53−7.44 (m, 2H), 7.06 (q, J = 8.9 Hz, 2H), 4.85−4.79 (m, 1H), 4.62−4.49 (m, 1H), 4.21−4.02 (m, 2H), 3.55−3.42 (m, 3H), 2.01−1.89 (m, 3H).

*3,3,3-Trifluoro-2-{[4-(4-fluorophenyl)-5-methoxycarbonyl-4-methyl-2-thiazol-2-yl-1H-pyrimidin-6-yl]methoxy}propanoic acid (**31w**)*. MS: calcd (MH^+) 488.1, exp (MH^+) 488.1. HRMS: calcd (MH^+) 488.0898, exp (MH^+) 488.0897. ^{1}H NMR (Methanol-d_4) δ 7.93 (d, J = 3.0 Hz, 1H), 7.73 (d, J = 3.3 Hz,

1H), 7.55−7.47 (m, 2H), 7.05 (t, J = 8.8 Hz, 2H), 4.85−4.74 (m, 2H), 4.39 (q, J = 7.8 Hz, 1H), 3.45 (s, 3H), 1.94 (s, 3H).

General Procedures for the Synthesis of Amino Acid-substituted Analogues 34a−f. Analogues **34a−f** was synthesized in analogy to **31a−t** by using enantiomer (*S*)-**7a** and chiral amino esters as starting materials. (*S*)-**7a** was obtained by chiral SFC separation of **7a** in 48% yield. To a solution of (*S*)-**7a** (6.91 g, 20 mmol) and DMAP (3.66 g, 30 mmol) in 200 mL of DCM was added Boc_2O (5.46 g, 25 mmol), and the mixture was stirred overnight. The organic phase was washed with water and brine, dried over anhydrous Na_2SO_4 and concentrated. The residue was purified by flash chromatography to afford the *N*-Boc protected intermediate, which was then dissolved in 300 mL of CCl_4. To this solution was added NBS (3.56 g, 20 mmol) and AIBN (100 mg) and the mixture was stirred at 50 ℃ for 2 h. The reaction mixture was washed with water, dried over anhydrous Na_2SO_4 and concentrated. The residue was purified by flash chromatography to give bromide intermediate in 82% yield over 2 steps.

To a mixture of this bromide (1.05 g, 2.0 mmol) and K_2CO_3 (0.7 g) in 10 mL of DMF was added amino ester **35** (2.0 mmol), and the mixture was stirred at 40 ℃ for 3 h before it was partitioned between water and EtOAc. The organic phase was washed with brine, dried over anhydrous Na_2SO_4 and concentrated. The residue was purified by flash chromatography to give **36** in > 80% yield. A mixture of **36** (1.0 mmol) and LiOH (10.0 mmol) in 10 mL of MeOH/H_2O was stirred at rt for 2 h. When the hydrolysis was complete, the mixture was extracted with EtOAc and the organic phase was washed with brine, dried over anhydrous Na_2SO_4 and concentrated. The residue was dissolved in 10 mL of DCM and to this solution was added 1 mL of TFA. The reaction mixture was stirred at rt for 2 h before partitioned between DCM and water. The organic phase was washed with brine, dried over anhydrous Na_2SO_4 and concentrated. Analogues **34a−e** were purified and obtained as powder in > 70% yields.

*(2S)-4,4-Difluoro-1-[[(4S)-4-(4-fluorophenyl)-5-methoxycarbonyl-4-methyl-2-thiazol-2-yl-1H-pyrimidin-6-yl]methyl]pyrrolidine-2-carboxylic acid (**34a**).* $[\alpha]_D^{20}$ = 56.0 (1.05 mg/mL, MeOH). MS: calcd (MH^+) 495.1, exp (MH^+) 495.1. HRMS: calcd (MH^+) 495.1308, exp (MH^+) 495.1315. ^{1}H NMR (Methanol-d_4) δ 8.22 (m, 2H), 7.68−7.65 (m, 2H), 7.21−7.17 (m, 2H), 4.16 (d, *J* = 15.6 Hz, 1H), 4.02 (t, *J* = 8.0 Hz, 1H), 3.93 (d, *J* = 15.6 Hz, 1H), 3.72−3.61 (m, 1H), 3.53 (s, 3H), 3.29−3.19 (m, 1H), 2.91−2.78 (m, 1H), 2.59−2.55 (m, 1H), 2.17 (s, 3H).

*(S)-4-[(S)-6-(4-Fluoro-phenyl)-5-methoxycarbonyl-6-methyl-2-thiazol-2-yl-3,6-dihydro-pyrimidin-4-ylmethyl]-morpholine-3-carboxylic acid (**34b**).* $[\alpha]_D^{20}$ = 8.4 (1.0 mg/mL, MeOH). MS: calcd (MH^+) 475.1, exp (MH^+) 475.1. HRMS: calcd (MH^+) 475.1446, exp (MH^+) 475.1449. ^{1}H NMR (Methanol-d_4) δ 8.07 (d, *J* = 3.0 Hz, 1H), 7.97 (d, *J* = 3.2 Hz, 1H), 7.64−7.58 (m, 2H), 7.12 (t, *J* = 8.8 Hz, 2H), 4.33−4.25 (m, 2H), 4.13 (dd, *J* = 4.4, 2.7 Hz, 2H), 3.98−3.86 (m, 3H), 3.59−3.52 (m, 1H), 3.51−3.48 (m, 3H), 3.01 (ddd, *J* = 12.4, 5.7, 3.3 Hz, 1H), 2.10−2.06 (m, 3H).

*(2R)-4,4-Difluoro-1-{[(4S)-4-(4-fluorophenyl)-5-methoxycarbonyl-4-methyl-2-thiazol-2-yl-1H-pyrimidin-6-yl]methyl}pyrrolidine-2-carboxylic acid (**34c**).* $[\alpha]_D^{20}$ = 20.0 (0.95 mg/mL, MeOH). MS: calcd (MH^+) 495.1, exp (MH^+) 495.1. HRMS: calcd (MH^+) 495.1308, exp (MH^+) 495.1310. ^{1}H NMR (Methanol-d_4) δ 8.00 (d, *J* = 3.0 Hz, 1H), 7.87 (d, *J* = 2.8 Hz, 1H), 7.56 (dd, *J*= 8.8, 5.3 Hz, 2H), 7.10 (t, *J* = 8.9 Hz, 2H), 4.10 (d, *J* = 15.3 Hz, 1H), 4.00−3.92 (m, 2H), 3.66−3.57 (m, 2H), 3.48 (s, 3H), 2.85−2.77 (m, 1H), 2.58−2.50 (m, 1H), 1.99 (s, 3H).

*(R)-4-[(S)-6-(4-Fluoro-phenyl)-5-methoxycarbonyl-6-methyl-2-thiazol-2-yl-3,6-dihydro-pyrimidin-4-ylmethyl]-morpholine-3-carboxylic acid (**34d**).* $[\alpha]_D^{20}$ = 25.3 (0.9 mg/mL, MeOH). MS: calcd (MH^+) 475.1, exp (MH^+) 475.1. HRMS: calcd (MH^+) 475.1446, exp (MH^+) 475.1455. ^{1}H NMR (Methanol-d_4) δ 8.07 (d, *J* = 3.0 Hz, 1H), 7.98 (d, *J* = 3.3 Hz, 1H), 7.65−7.57 (m, 2H), 7.12 (t, *J* = 8.8 Hz, 2H), 4.29 (q, *J* = 16.2 Hz, 2H), 4.19−4.06 (m, 2H), 3.99−3.84 (m, 3H), 3.57−3.51 (m, 1H), 3.49 (s, 3H), 3.02 (ddd, *J* = 12.4, 6.1, 3.2 Hz, 1H), 2.09 (s, 3H).

*(2S)-1-[[(4S)-4-(4-Fluorophenyl)-5-methoxycarbonyl-4-methyl-2-thiazol-2-yl-1H-pyrimidin-6-yl]methyl]pyrrolidine-2-carboxylic acid (**34e**)*. MS: calcd (MH^+) 459.3, exp (MH^+) 459.1. ^{1}H NMR (Methanol-d_4) δ 7.96 (dd, J = 3.1, 1.6 Hz, 1H), 7.86 (dd, J = 3.0, 1.8 Hz, 1H), 7.71−7.51 (m, 2H), 7.18−7.03 (m, 2H), 4.61−4.46 (m, 1H), 4.41−4.30 (m, 1H), 4.27−4.15 (m, 1H), 3.93 (m, 2H), 3.49 (m, 2H), 3.15 (m, 1H), 2.64−2.45 (m, 2H), 2.36−2.15 (m, 1H), 2.12−1.92 (m, 4H).

*Methyl (4S)-6-[[(2S)-4,4-Difluoro-2-methoxycarbonyl-pyrrolidin-1-yl]methyl]-4-(4-fluorophenyl)-4-methyl-2-thiazol-2-yl-1H-pyrimidine-5-carboxylate (**34f**)*. To a solution of **36** (W = -CF_2-, 0.5 mmol) in 5 mL of DCM was added 0.5 mL of TFA, and the reaction mixture was stirred at rt for 2 h before partitioned between water and DCM. The aqueous phase was extrated with DCM and the combined organic phase was washed with water and brine, dried over anhydrous Na_2SO_4 and concentrated. The residue was purified by prep-HPLC to afford analogue **34f** as powder in 85% yield. MS: calcd (MH^+) 509.1, exp (MH^+) 509. HRMS: calcd (MH^+) 509.1465, exp (MH^+) 509.1466. ^{1}H NMR (Methanol-d_4) δ 8.26−8.21 (m, 2H), 7.69−7.62 (m, 2H), 7.23−7.13 (m, 2H), 4.15−4.07 (m, 1H), 4.02 (dd, J = 7.3, 8.8 Hz, 1H), 3.96−3.90 (m, 1H), 3.82 (s, 3H), 3.65−3.54 (m, 1H), 3.53 (s, 3H), 3.28−3.13 (m, 1H), 2.89−2.74 (m, 1H), 2.61−2.44 (m, 1H), 2.22−2.14 (m, 3H).

Microsomal Stability Assay. Each incubated mixture contained 0.5 mg/mL liver microsome (human or mouse), 100 mM potassium phosphate buffer (pH 7.4), 10 mM NADPH, and 1 μM test compound in a total volume of 400 μL. After prewarming at 37 ℃ for 10 min, the NADPH was added to initiate the reaction. The reaction was terminated after 0, 3, 6, 9, 15, or 30 min by adding 150 μL of 100 ng/mL tolbutamide (internal standard) in ice-cold methanol into 300 μL of incubation mixture. The sample was then centrifuged at 4000 rpm for 10 min at 4 ℃. The supernatant was then analyzed by LC−MS/MS.

LYSA Solubility Assay. A 150 μL aliquot of 10 mM DMSO stock solution of the compound was prepared and divided into two portions. For one portion, the DMSO solution was evaporated to dryness at 35 ℃ in a centrifugal vacuum evaporator from Genevac Technologies, and the residue was

redissolved in 50 mM phosphate buffer (pH 6.5). The mixture was stirred and shaken for 1−2 h. The solution was allowed to stand overnight and then filtered before HPLC analysis. The other portion was used to prepare a calibration curve by dilution of the DMSO stock solution using the same PBS buffer mentioned above to obtain a series of solutions with concentrations in the range of 50−500 μM.

Biology General Comments. Brief descriptions of the biological protocols used to generate data in this study can be found below. Cells and culture conditions: HepDE19 cells were derived from HepG2 cells (ATCC) through transfection with pTet-off plasmid (Clontech) that expresses the Tet-responsive transcriptional activator and pTREHBVDE plasmid in which HBV pgRNA expression is controlled by a tetracycline-responsive CMV promoter.[19, 25] The transfected cells were selected with G418 (Invitrogen). In tetracycline-free medium, cells support high levels of HBV DNA replication and HBV virus secretion. Caco-2 cells were obtained from ATCC and the measurement of compound permeability was carried out according to reported procedures. pcDNA3.1HBV1.1mer plasmid was prepared by Qiagen EndoFree Plasmid Giga Kit. All of the animal studies including DMPK evaluations and the HDI mouse model were approved and regularly reviewed by the Institutional Animal Care and Use Committee (IACUC) of Roche Pharma Research and Early Development (pRED) China.

Anti-HBV Activity and Cytotoxicity: HepDE19 cells were seeded into 96-well plates (3×10^4 cells/well) with tetracycline-free medium and incubated overnight at 37 ℃. The test or control compounds were half-log diluted serially with medium and added into the plates with 0.5% of final DMSO concentration. After 5 d incubation, cells were washed with PBS and lysed with 50 mM Tris-1mM EDTA-0.2% CA-630 (pH 8.0) at 37 ℃ for 20 min. After centrifugation to remove nuclei and other debris, the supernatant was transferred into a new plate and incubated with 2M NaOH/20×SSC (3M NaCl, 0.3M Sodium citrate, pH7.0) at rt for 30 min. Then the samples were transferred to nylon membrane and neutralized with 1M Tris (pH7.4)/2M NaCl. The presence of HBV DNA was detected by dot-blot with DIG-labeled HBV specific DNA probes and quantified by dot density. To determine

the cytotoxicity of test compounds, HepDE19 cells (5×10^3 cells/well) were seeded into 96-well plates and incubated with compounds as described above. Five days after treatment, cell viability was measured by addition of 20 μl of CCK-8 reagent. After 4 h incubation at 37 ℃, the absorbance at wavelengths of 450 nm and 630 nm (OD_{450} and OD_{630}) was recorded by a plate reader.

Protein expression and purification. HBc1−149 Y132A construct was cloned as described previously.[26] The recombinant protein was expressed in *Escherichia coli* strain BL21(DE3) and purified by Ni affinity column followed by anion-exchange chromatography. The His6 tag was removed by using tobacco etch virus (TEV) protease. Then the tagless HBc1−149 Y132A protein with additional C-terminal ENLYFQ was dialyzed into 25 mM Tris buffer (pH 9.0) containing 2 mM DTT and 10 mM EDTA. Finally the product was concentrated and stored at −80 ℃.

Crystallization and structure determination. Sitting drop was setup using equal volume of HBc1−149 Y132A (17 mg/mL) in 20 mM Tris buffer (pH 9.0), 2 mM DTT and crystallization buffer containing 100 mM citrate (pH 5.6), 21% (vol/vol) isopropanol, 1% (wt/vol) PEG 10,000 at 20 ℃. Apo crystal was soaked in the crystallization buffer plus 25% glycerol and 2mM of **34a** for 2 h before it was flash frozen in liquid nitrogen. The dataset was collected on single crystal for Y132A-**34a** complex structure at BL17U beamline, Shanghai Synchrotron Radiation Facility. Data were processed by using HKL2000[27]. The structure was solved by PHASER[28] molecular replacement using 4BMG as the search model. The model was manually built and refined several rounds by using PHENIX package[29] and COOT[30]. The final model quality was evaluated by MolProblity[31] (Table S1).

Pharmacokinetic (PK) Analysis. All of the compounds were evaluated in CD-1 mice (18−25 g; three mice in each group were used for blood collection at each time point). Compounds were dissolved in 6% Solutol solution (Solutol: Ethanol, 1:1, v/v), and 94% 0.9% saline for i.v. dose and 1% RC591 for oral dose. In each species, blood samples (150 μL) were collected at eight time points (p.o.) or nine time points (i.v.) into sodium heparin centrifuge tubes, and plasma samples were then isolated by centrifugation and stored at −20 °C prior to analysis. Plasma concentrations were determined by

LC−MS/MS, and the data were analyzed by noncompartmental methods using WinNonlin Pro (Pharsight Corp., Mountain View, CA).

In vivo Efficacy in HDI Mouse Model. Female BALB/c mice (6-8 weeks old) were injected through tail vein with 20 μg plasmid pcDNA3.1HBV encoding a 1.1-mer HBV genome (Genotype D) in a volume of normal saline equivalent to 8% of the mouse body weight. The total volume was delivered within a few seconds. 7 h post injection, mice were orally dosed by blank vehicle, 0.1 mg/kg of entecavir, or 12.5 mpk, 25 mpk and 50 mpk of **34a** at indicated frequency for 5 days, respectively. Plasma and liver samples were collected at the indicated time points for HBV DNA quantification by real-time PCR.

SUPPORTING INFORMATION

Detailed experimental procedures for the synthesis of key intermediates including amidines **12**, 4,4-difluoroproline methyl ester, and *t*-butyl ester **20**. X-ray structure of (*S*)-**7a**. Data collection and refinement statistics of Y132A-**34a** co-crystal structure. CYP inhibition, plasma protein binding assay, and mechanistic studies of **34a** to the capsid assembly by size-exclusion chromatography (SEC) and transmission electron microscopy (TEM). This material is available free of charge via the Internet at http://pubs.acs.org.

AUTHOR INFORMATION

Corresponding Author

* Phone: +86 21 28946723. E-mail: gordon.tang@roche.com.

Notes

The authors declare no competing financial interest.

ACKNOWLEDGEMENTS

We are grateful to Qinshan Gao, Wenzhi Cheng, and Liqin Chen for purification of final compounds and analytical assistance, Jason C. Wong for scientific discussions, and Feng Yu and Jianhua He at the Shanghai Synchrotron Radiation Facility for assistance on X-ray data collection.

ABBREVIATIONS USED

AIBN, azobisisobutyronitrile; CDI, *N*, *N'*-carbonyldiimidazole; DMAP, *N*, *N'*-dimethylaminopyridine; GSH, glutathione; HAP, heteroaryldihydropyrimidine; HATU, 2-(7-aza-1H-benzotriazole-1-yl)-1,1,3,3-tetramethyluronium hexafluorophosphate; HB, hydrogen-bonding; HBeAg, hepatitis B e-antigen; HBV, hepatitis B virus; HDI, hydrodynamic injected; hERG, human ether-a-go-go related gene; HLM, human liver microsome; IFN, interferon; LYSA, lyophilized solubility assay; MLM, mouse liver microsome; MNT, micronucleus test; mpk, mg/kg or milligram per kilogram; NBS, N-bromosuccinimide; NMP, N-methyl-2-pyrrolidone; pgRNA, pre-genomic RNA; PPA, polyphosphoric acid; PSA, polar surface area; SAR, structure−activity relationship; SFC, supercritical fluid chromatography; SDPK, single dose pharmacokinetics; SPR, structure−property relationship; PCR, polymerase chain reaction; TFA, trifluoroacetic acid; TFAA, trifluoroacetic acid anhydride; VDW, van der Waals.

PDB (5GMZ) of **34a**: Authors will release the atomic coordinates and experimental data upon article publication.

REFERENCES

1. You, C. R.; Lee, S. W.; Jang, J. W.; Yoon, S. K. Update on hepatitis B virus infection. *World J. of Gastroenterol.* **2014**, *20*, 13293−13305.

2. Hadziyannis, S. J. Update on hepatitis B virus infection: focus on treatment. *J. Clin. Transl. Hepatol.* **2014**, *2*, 285−291.

3. Baltayiannis, G.; Karayiannis, P. Treatment options beyond IFNalpha and NUCs for chronic HBV infection: expectations for tomorrow. *J. Viral Hepat.* **2014**, *21*, 753−761.

4. Orlando, R.; Foggia, M.; Maraolo, A. E.; Mascolo, S.; Palmiero, G.; Tambaro, O.; Tosone, G. Prevention of hepatitis B virus infection: from the past to the future. *Eur. J. Clin. Microbiol. Infect. Dis.* **2015**, *34*, 1059−1070.

5. Packianathan, C.; Katen, S. P.; Dann, C. E., 3rd; Zlotnick, A. Conformational changes in the hepatitis B virus core protein are consistent with a role for allostery in virus assembly. *J. Virol.* **2010**, *84*, 1607−1615.

6. Zlotnick, A.; Venkatakrishnan, B.; Tan, Z.; Lewellyn, E.; Turner, W.; Francis, S. Core protein: A pleiotropic keystone in the HBV lifecycle. *Antiviral Res.* **2015**, *121*, 82−93.

7. Deres, K.; Schroder, C. H.; Paessens, A.; Goldmann, S.; Hacker, H. J.; Weber, O.; Kramer, T.; Niewohner, U.; Pleiss, U.; Stoltefuss, J.; Graef, E.; Koletzki, D.; Masantschek, R. N.; Reimann, A.; Jaeger, R.; Gross, R.; Beckermann, B.; Schlemmer, K. H.; Haebich, D.; Rubsamen-Waigmann, H. Inhibition of hepatitis B virus replication by drug-induced depletion of nucleocapsids. *Science* **2003**, *299*, 893−896.

8. Bourne, C. R.; Finn, M. G.; Zlotnick, A. Global structural changes in hepatitis B virus capsids induced by the assembly effector HAP1. *J. Virol.* **2006**, *80*, 11055−11061.

9. Brezillon, N.; Brunelle, M. N.; Massinet, H.; Giang, E.; Lamant, C.; DaSilva, L.; Berissi, S.; Belghiti, J.; Hannoun, L.; Puerstinger, G.; Wimmer, E.; Neyts, J.; Hantz, O.; Soussan, P.; Morosan, S.; Kremsdorf, D. Antiviral activity of Bay 41-4109 on hepatitis B virus in humanized Alb-uPA/SCID mice. *Plos One* **2011**, *6*, e25096.

10. Shi, C.; Wu, C. Q.; Cao, A. M.; Sheng, H. Z.; Yan, X. Z.; Liao, M. Y. NMR-spectroscopy-based metabonomic approach to the analysis of Bay41-4109, a novel anti-HBV compound, induced hepatotoxicity in rats. *Toxicol. Lett.* **2007**, *173*, 161−167.

11. Wu, G.; Liu, B.; Zhang, Y.; Li, J.; Arzumanyan, A.; Clayton, M. M.; Schinazi, R. F.; Wang, Z.; Goldmann, S.; Ren, Q.; Zhang, F.; Feitelson, M. A. Preclinical characterization of GLS4, an inhibitor of hepatitis B virus core particle assembly. *Antimicrob. Agents Chemother.* **2013**, *57*, 5344−5354.

12. Klumpp, K.; Lam, A. M.; Lukacs, C.; Vogel, R.; Ren, S.; Espiritu, C.; Baydo, R.; Atkins, K.; Abendroth, J.; Liao, G.; Efimov, A.; Hartman, G.; Flores, O. A. High-resolution crystal structure of a hepatitis B virus replication inhibitor bound to the viral core protein. *P. Natl. Acad. Sci. U.S.A.* **2015**, *112*, 15196−15201.

13. Wang, X. Y.; Wei, Z. M.; Wu, G. Y.; Wang, J. H.; Zhang, Y. J.; Li, J.; Zhang, H. H.; Xie, X. W.; Wang, X.; Wang, Z. H.; Wei, L.; Wang, Y.; Chen, H. S. In vitro inhibition of HBV replication by a novel compound, GLS4, and its efficacy against adefovir-dipivoxil-resistant HBV mutations. *Antiviral Ther.* **2012**, *17*, 793−803.

14. Delaney, W. E.; Edwards, R.; Colledge, D.; Shaw, T.; Furman, P.; Painter, G.; Locarnini, S. Phenylpropenamide derivatives AT-61 and AT-130 inhibit replication of wild-type and lamivudine-resistant strains of hepatitis B virus in vitro. *Antimicrob. Agents Chemother.* **2002**, *46*, 3057−3060.

15. Wang, P.; Naduthambi, D.; Mosley, R. T.; Niu, C.; Furman, P. A.; Otto, M. J.; Sofia, M. J. Phenylpropenamide derivatives: anti-hepatitis B virus activity of the Z isomer, SAR and the search for novel analogs. *Bioorg. Med. Chem. Lett.* **2011**, *21*, 4642−4647.

16. Campagna, M. R.; Liu, F.; Mao, R.; Mills, C.; Cai, D.; Guo, F.; Zhao, X.; Ye, H.; Cuconati, A.; Guo, H.; Chang, J.; Xu, X.; Block, T. M.; Guo, J. T. Sulfamoylbenzamide derivatives inhibit the assembly of hepatitis B virus nucleocapsids. *J. Virol.* **2013**, *87*, 6931−6942.

17. Yang, L.; Shi, L. P.; Chen, H. J.; Tong, X. K.; Wang, G. F.; Zhang, Y. M.; Wang, W. L.; Feng, C. L.; He, P. L.; Zhu, F. H.; Hao, Y. H.; Wang, B. J.; Yang, D. L.; Tang, W.; Nan, F. J.; Zuo, J. P.

Isothiafludine, a novel non-nucleoside compound, inhibits hepatitis B virus replication through blocking pregenomic RNA encapsidation. *Acta Pharmacol. Sin.* **2014**, *35*, 410−418.

18. Katen, S. P.; Chirapu, S. R.; Finn, M. G.; Zlotnick, A. Trapping of hepatitis B virus capsid assembly intermediates by phenylpropenamide assembly accelerators. *ACS Chem. Biol.* **2010**, *5*, 1125−1136.

19. Mao, R.; Zhang, J.; Jiang, D.; Cai, D.; Levy, J. M.; Cuconati, A.; Block, T. M.; Guo, J. T.; Guo, H. Indoleamine 2,3-dioxygenase mediates the antiviral effect of gamma interferon against hepatitis B virus in human hepatocyte-derived cells. *J. Virol.* **2011**, *85*, 1048−1057.

20. Beno, B. R.; Yeung, K. S.; Bartberger, M. D.; Pennington, L. D.; Meanwell, N. A. A survey of the role of noncovalent sulfur interactions in drug design. *J. Med. Chem.* **2015**, *58*, 4383−4438.

21. Halgren, T. A. Merck molecular force field. I. Basis, form, scope, parameterization, and performance of MMFF94. *J. Comput. Chem.* **1996**, *17*, 490−519.

22. Bourne, C.; Lee, S.; Venkataiah, B.; Lee, A.; Korba, B.; Finn, M. G.; Zlotnick, A. Small-molecule effectors of hepatitis B virus capsid assembly give insight into virus life cycle. *J. Virol.* **2008**, *82*, 10262−10270.

23. Zhang, J.; Blazecka, P. G.; Angell, P.; Lovdahl, M.; Curran, T. T. Indium(III) mediated Markovnikov addition of malonates and beta-ketoesters to terminal alkynes and the formation of Knoevenagel condensation products. *Tetrahedron* **2005**, *61*, 7807−7813.

24. Huang, L. R.; Gabel, Y. A.; Graf, S.; Arzberger, S.; Kurts, C.; Heikenwalder, M.; Knolle, P. A.; Protzer, U. Transfer of HBV genomes using low doses of adenovirus vectors leads to persistent infection in immune competent mice. *Gastroenterology* **2012**, *142*, 1447−1450.

25. Guo, H.; Jiang, D.; Zhou, T.; Cuconati, A.; Block, T.; Guo, J. Characterization of the intracellular deproteinized relaxed circular DNA of hepatitis B virus: an intermediate of covalently closed circular DNA formation. *J. Virol.* **2007**, *81*, 12472−12484.

26. Alexander, C. G.; Jürgens, M. C.; Shepherd, D. A.; Freund, S. M. V.; Ashcroft, A. E.; Ferguson, N. Thermodynamic origins of protein folding, allostery, and capsid formation in the human hepatitis B virus core protein. *P. Natl. Acad. Sci. U.S.A.* **2013**, *110*, E2782−E2791.

27. Otwinowski, Z.; Minor, W. Processing of X-ray diffraction data collected in oscillation mode. *Methods Enzymol.* **1997**, *276*, 307−326.

28. McCoy, A. J.; Grosse-Kunstleve, R. W.; Adams, P. D.; Winn, M. D.; Storoni, L. C.; Read, R. J. Phaser crystallographic software. *J. Appl. Crystallogr.* **2007**, *40*, 658−674.

29. Adams, P. D.; Afonine, P. V.; Bunkoczi, G.; Chen, V. B.; Davis, I. W.; Echols, N.; Headd, J. J.; Hung, L.-W.; Kapral, G. J.; Grosse-Kunstleve, R. W.; McCoy, A. J.; Moriarty, N. W.; Oeffner, R.; Read, R. J.; Richardson, D. C.; Richardson, J. S.; Terwilliger, T. C.; Zwart, P. H. PHENIX: a comprehensive Python-based system for macromolecular structure solution. *Acta Crystallogr., Sect. D: Biol. Crystallogr.* **2010**, *66*, 213−221.

30. Emsley, P.; Cowtan, K. Coot: model-building tools for molecular graphics. *Acta Crystallogr., Sect. D: Biol. Crystallogr.* **2004**, *60*, 2126−2132.

31. Chen, V. B.; Arendall, W. B.; Headd, J. J.; Keedy, D. A.; Immormino, R. M.; Kapral, G. J.; Murray, L. W.; Richardson, J. S.; Richardson, D. C. MolProbity: all-atom structure validation for macromolecular crystallography. *Acta Crystallogr., Sect. D: Biol. Crystallogr.* **2010**, *66*, 12−21.

Table of Contents graphic

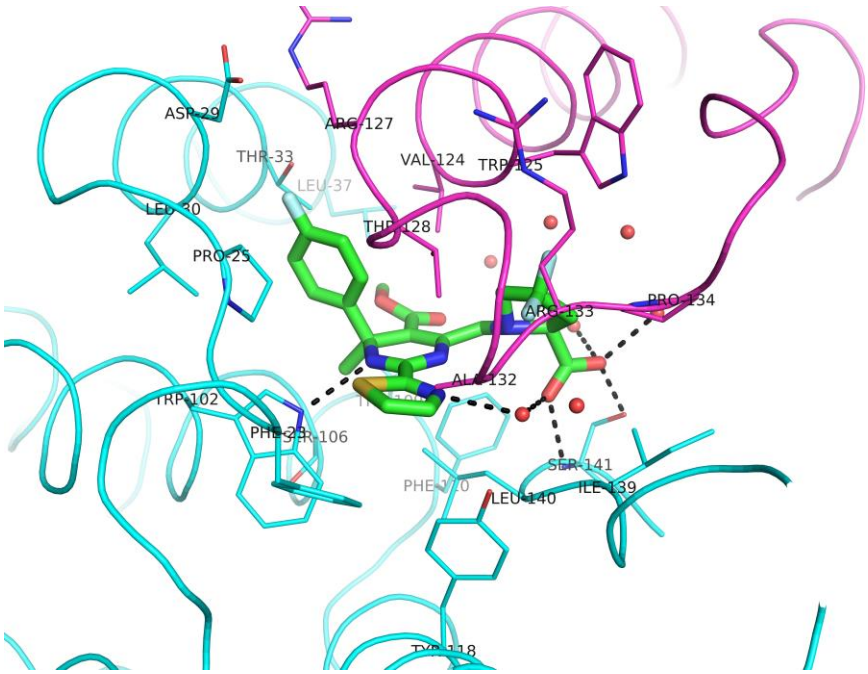

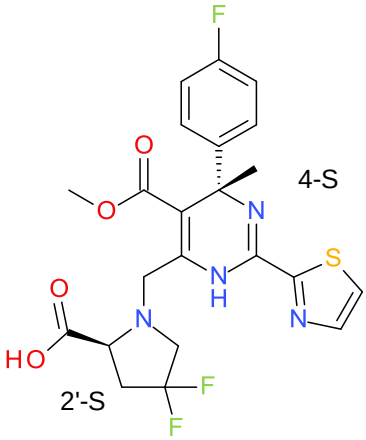

34a (4-methyl HAP)

EC_{50}: 0.084 μM

CC_{50}: 160 μM (HepDE19)